Zootaxa 5375 (3): 349–378
https://www.mapress.com/zt/

Article

ISSN 1175-5326 (print edition)
ZOOTAXA
ISSN 1175-5334 (online edition)

https://doi.org/10.11646/zootaxa.5375.3.3
http://zoobank.org/urn:lsid:zoobank.org:pub:4EBF95D8-B03D-4859-B127-AD0840DA10FB

How complex is the *Naineris setosa* species complex? First integrative study of a presumed cosmopolitan and invasive annelid (Sedentaria: Orbiniidae)

RICARDO ÁLVAREZ [1,*] & NATALIYA BUDAEVA [2]

[1] *Graduate program in Oceanic Coastal Systems (PGSISCO), Federal University of Paraná, Pontal do Paraná, Paraná, Brazil.*
https://orcid.org/0000-0002-3509-0187

[2] *Department of Natural History, University Museum of Bergen, University of Bergen, Allégaten 41, 5007 Bergen, Norway*
nataliya.budaeva@uib.no; https://orcid.org/0000-0001-9748-2285

* *Corresponding author: ricastralvarez@gmail.com*

Abstract

We performed a comparative study of the specimens from the *Naineris setosa* complex from the Pacific and the Atlantic Oceans and re-described the syntype of *N. setosa*, including the selection of the lectotype. Molecular phylogenetic and species delimitation analyses based on two mitochondrial (COI and 16S) and one nuclear (28S) marker revealed the presence of three species. One clade with wide Amphi-Atlantic distribution was attributed as *Naineris setosa* s. str. The second Atlantic clade restricted to Southern and Southeastern Brazil was described as a new species, *Naineris lanai* sp. n. The third clade, reported from the Northwestern Pacific, was identified as a new species but was not formally described due to the presence of only juvenile-sized worms in the studied material. Detailed morphological descriptions of several diagnostic characters in the *Naineris setosa* complex are provided.

Key words: Integrative taxonomy, 28S rRNA gene, mtDNA COI, 16S, cosmopolitanism, new species.

Introduction

Naineris setosa (Verril, 1900) is a "cosmopolitan" orbiniid species originally described from intertidal shell-sand sediment in Bermuda. Due to the apparent lack of consistent morphological differences among its records, *N. setosa* was for decades assumed to have an Amphi-American distribution with records both from the East Pacific (Dean & Blake 2015; Blake 2017) and the Atlantic (Treadwell 1901; Hartman 1951; 1957; Rioja 1960; Solis-Weiss & Fauchald 1989; Amaral *et al*. 2006; Blake & Giangrande 2011). It is currently known that truly widespread annelids are rare (Hutchings & Kupriyanova 2018). One of such cases has been confirmed within orbiniids for a small, presumably invasive species, *Proscoloplos cygnochaetus* Day, 1954, and its extremely wide distribution was explained by its capacity to anchor on vessels using mucous glands and chaetae possibly in combination with architomic reproduction (Meyer *et al.* 2008). Several species of *Naineris* Blainville, 1828 currently have cosmopolitan status. Nevertheless, this should be tested based on a combination of molecular data and comparative morphological studies.

Naineris setosa is unique in lacking uncini and subuluncini in thoracic neuropodia, which makes it similar to *Leitoscoloplos* Day, 1977 and *Scoloplella* Day, 1963, but it has a rounded prostomium as in all other species of *Naineris*. Hartman (1957) equivocally considered *N. setosa* related to *Leitoscoloplos* based on the presence of only crenulated capillaries in thoracic neuropodia. Several attempts were made to reconstruct the phylogeny of Orbiniidae and to assess the position of *Naineris* among other genera. Blake (2000) proposed a phylogeny based on the morphological characters and recovered *Naineris* as a paraphyletic genus. Bleidorn *et al*. (2005, 2009) confirmed the monophyly of *Naineris* + *Protoaricia* based on molecular data suggesting a progenetic origin for *Protoaricia* either within or as a sister to *Naineris*. However, their most advanced analysis based on six markers included only three species of the genus, the type species *Naineris quadricuspida* (Fabricius, 1780), *Naineris dendritica* (Kinberg, 1867), and *Naineris laevigata* (Grube, 1855). Later, Zhadan *et al*. (2015) proposed several phylogenetic reconstructions of Orbiniidae based on three individual markers. They included four species of *Naineris* and

Accepted by W. Magalhães: 31 Oct. 2023; published: 23 Nov. 2023

recovered the genus as paraphyletic or monophyletic, depending on the marker analyzed. No combined analysis was presented in the study, and the monophyletic status of the genus could not be assessed based on the combined dataset. Nevertheless, none of the phylogenetic studies included *N. setosa* in the analyses, and its phylogenetic placement within *Naineris* remains unclear.

Even though most of the confirmed invasive polychaetes belong to Serpulidae and Spionidae, some orbiniids, such as *Scoloplos capensis* (Day, 1961), *Leitoscoloplos kerguelensis* (McIntosh, 1885), and *Naineris quadraticeps* Day, 1965 were also considered as invasive (Çinar 2013). *Naineris setosa* was repeatedly reported as an invasive species in the Mediterranean region (Blake & Giangrande 2011; Khedhri *et al*. 2014; Dean & Blake 2015; Atzori *et al*. 2016); however, because none of the studies was supported by molecular data, the species should be considered as cryptogenic.

In the present study, we re-examine the type material of *N. setosa* herein designated as lectotype according to Article 74 (ICZN 1999) and perform morphological and molecular analyses of the specimens collected from various localities in the Western Atlantic, the Mediterranean, and the Northeast Pacific. Based on the results, we explore this species' genetic and morphological diversity and describe one new species from Southern and Southeastern Brazil.

Material and methods

Sampling

Specimens of the *Naineris setosa* species complex were collected intertidally along the Brazilian coast from 2020 to 2022 from Santa Catarina to Pernambuco states in different estuarine beaches, from bays and embayments (Fig. 1). The geographical localities of the collected samples are listed in Table 1. To avoid the common fragmentation of the specimens, they were sorted, anesthetized with 8% magnesium chloride in seawater, and preserved in either 4% formalin or 99.5% ethanol directly in the field. Formalin-fixed samples were subsequently transferred into 70% ethanol.

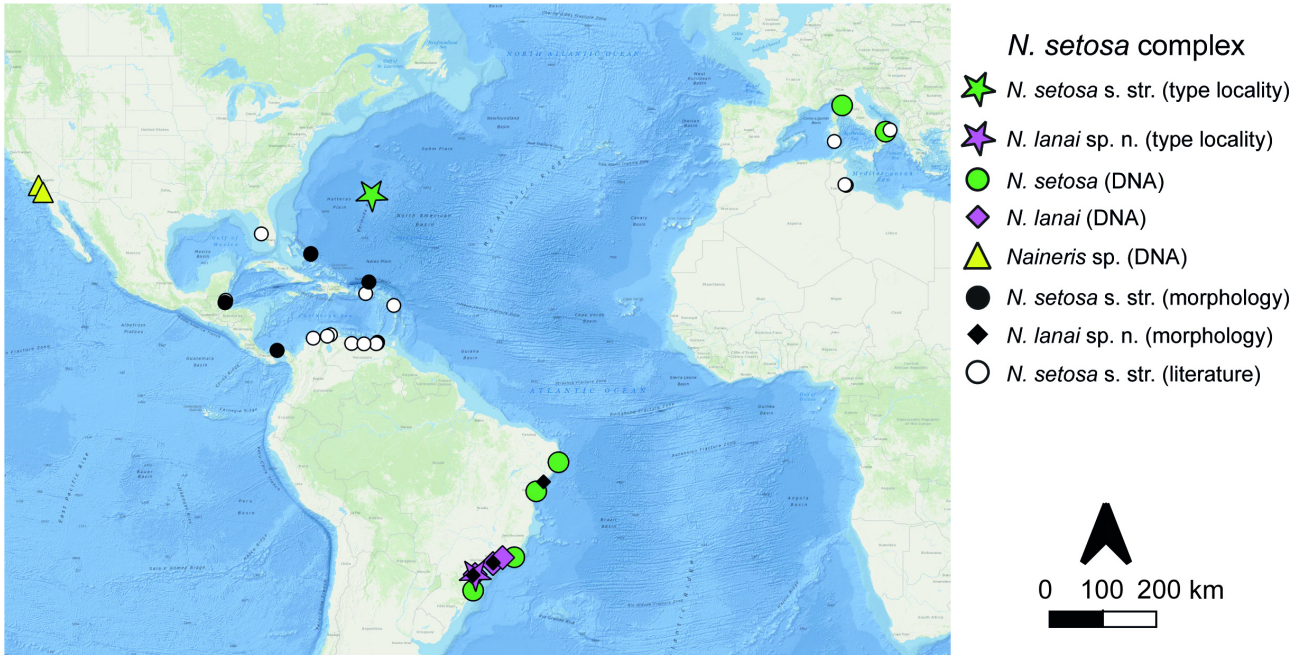

FIGURE 1. Distribution of the *Naineris* species described in this study.

Morphological study

The specimens were studied using a Leica MZ stereomicroscope and a Leica DM 6000 B compound microscope. Digital photos were made with a Leica M205C stereomicroscope with a digital camera Leica DMC5400 attached and combined with the Z-stack function using Leica LAS software. Methyl green and Shirlastain A dyes were

used for increasing contrast and visualizing external morphological structures. Thoracic and abdominal parapodia were dissected and mounted on slides in glycerol to examine the chaetal morphology and composition. Scanning Electron Microscopy (SEM) images were prepared in two institutions following different protocols. At the Center for Electron Microscopy, Federal University of Paraná, the Brazilian specimens stored in 70% ethanol were run through an increasing ethanol series, critical point dried in a Bal-tec CPD030 with ethanol as the transition fluid, mounted on an aluminum stub using double-sided tape, coated with a heavy metal, and examined using a Jeol JSM 6360-LV scanning electron microscope. At the University Museum of Bergen, University of Bergen, hexamethyldisilazane (HMDS) was used for specimen dehydration, which was then coated with gold and examined under a Zeiss FE-SEM model GEMINI, Supra 55VP.

Terminology follows the main revisions of the family (Hartman 1957; Blake 2017, 2020, 2021). Additionally, the following morphological characters were described. Thoracic ventral groove, a continuous well-defined groove along the ventral side of the thoracic segments, is described for the first time for *Naineris*. Ventral groove is common in abdominal segments in orbiniids, but its thoracic projection was not previously reported in the genus. Thoracic ventral longitudinal notches were discovered in specimens collected from muddy, possibly anoxic, sediments. They can almost reach consecutive annular rings or be less pronounced. Dorsal crest, following Blake (2017), is defined as ridges between abdominal branchiae. It may vary in shape from straight to folding and from inconspicuous to well-developed and can change in its shape along the body. Thoracic neuropodia can be of different shapes, varying from fleshy with rounded boundaries to thin and flattened with folding boundaries.

The segmental origin of branchiae and dorsal organs and the number of thoracic chaetigers were determined for 10 specimens from selected populations of the *N. setosa* complex from Brazil. Additionally, the following features were recorded at the chaetiger 50: total width disregarding parapodia (W), total length of branchiae (Bq), dorsal crest (DC), abdominal notopodial (NoL), and neuropodial lobes (NeL).

The redescription of *N. setosa* is based on the syntype labeled as *Aricia setosa* Verrill, 1900, deposited in the annelid collection of the Yale Peabody Museum, USA (YPM). In the present study, this specimen is designated as the lectotype. We also studied comparative materials from the Natural History Museum of Los Angeles County, USA (LACM-AHF Poly); the Smithsonian National Museum of Natural History, USA (USNM); the American Museum of Natural History, USA (AMNH); the Florida Museum, USA (FM); the reference collection of the Invasion laboratory at the Smithsonian Environmental Research Center, Maryland, USA (SERC); the Australian Museum, Australia (AM); Polychaeta Collection of the Museu Nacional, Universidade Federal do Rio de Janeiro, Brazil (MNRJP); Polychaeta Collection of the Museu de Diversidade Biológica, Instituto de Biologia, UNICAMP, Brazil (ZUEC-POL); Coleção Biológica Prof. Edmundo F. Nonato, Instituto Oceanográfico, Universidade de São Paulo, Brazil (ColBIO); the Invertebrate collection of the University Museum of Bergen, University of Bergen, Norway (ZMBN). The Brazilian specimens of *N. setosa* s. str. and type materials of *Naineris lanai* sp. n. are deposited in the MNRJ. Detailed information is provided in Table 1.

Molecular analyses

Thirty-five specimens from the *Naineris setosa* complex collected in the Eastern and Western Atlantic and the Northeastern Pacific were used for molecular analysis (Table 1). A single specimen of *Naineris aurantiaca* (Müller, 1858) from Pântano do Sul, Santa Catarina Island (Brazil), was used as an outgroup. Genomic DNA was extracted from ethanol-fixed tissue samples using 100 µL of QuickExtract™ solution, incubating in a thermocycler at 65 °C for 45 min, followed by 2 min at 90 °C. Fragments of a nuclear 28S rRNA and mitochondrial COI and 16S rRNA were amplified in a 25 µl reaction volume containing 2.5 µl 10x PCR buffer, 2 µl dNTP (2.5 mM), 1 µl forward and reverse primers (1 µM), 0.15 µl TaKaRa Taq (5 U/µl) with 1 µl template DNA, and double-distilled water. The primers and the PCR conditions are shown in Table 2. Obtained PCR products were run on 1% agarose gel for 30 min to visualize successful amplifications. The successful PCR products were sent to Macrogen Europe for purification and bidirectional Sanger sequencing (Applied Biosystems) using the same primers as in amplification. Contigs were automatically assembled from chromatograms for forward and reverse sequences and checked by eye in Geneious Prime (2023.1).

TABLE 1. List of specimens examined in the study with voucher museum numbers, localities, GenBank accession numbers for COI, 16S and 28S, Bold Sample and Process IDs.

Naineris	Voucher	Site	Coordinates	Collector	COI	16SrRNA	28SrRNA	BOLD Sample ID	BOLD Process ID
N. setosa s. str.	MNRJP 007629	Brazil, Santa Catarina	27.695°S; 48.565°W	R. Álvarez	OR732497	OR732526	OR732557	Alvarez_NS01	NAI001-23
N. setosa s. str.	MNRJP 007630	Brazil, Santa Catarina	27.695°S; 48.565°W	R. Álvarez	OR732496	OR732525	OR732556	Alvarez_NS02	NAI002-23
N. setosa s. str.	MNRJP 007631	Brazil, Santa Catarina	27.695°S; 48.565°W	R. Álvarez	OR732495	OR732524	OR732555	Alvarez_NS03	NAI003-23
N. setosa s. str.	MNRJP 007632	Brazil, Santa Catarina	27.695°S; 48.565°W	R. Álvarez	OR732494	OR732523	–	Alvarez_NS04	NAI004-23
N. setosa s. str.	MNRJP 007633	Brazil, Santa Catarina	27.695°S; 48.565°W	R. Álvarez	OR732493	OR732522	OR732554	Alvarez_NS05	NAI005-23
N. setosa s. str.	MNRJP 007628	Brazil, Santa Catarina	27.695°S; 48.565°W	R. Álvarez	–	–	–	–	–
N. setosa s. str.	MNRJP 007639	Brazil, Rio de Janeiro	22.882°S; 42.002°W	R. Álvarez	OR732492	–	OR732553	Alvarez_NS11	NAI006-23
N. setosa s. str.	MNRJP 007640	Brazil, Rio de Janeiro	22.882°S; 42.002°W	R. Álvarez	OR732491	OR732521	OR732552	Alvarez_NS12	NAI007-23
N. setosa s. str.	MNRJP 007641	Brazil, Rio de Janeiro	22.882°S; 42.002°W	R. Álvarez	OR732490	OR732520	OR732551	Alvarez_NS13	NAI008-23
N. setosa s. str.	MNRJP 007642	Brazil, Rio de Janeiro	22.882°S; 42.002°W	R. Álvarez	OR732489	OR732519	OR732550	Alvarez_NS14	NAI009-23
N. setosa s. str.	MNRJP 007643	Brazil, Rio de Janeiro	22.882°S; 42.002°W	R. Álvarez	OR732509	OR732537	OR732569	Alvarez_NS15	NAI010-23
N. setosa s. str.	MNRJP 007626	Brazil, Rio de Janeiro	22.882°S; 42.002°W	R. Álvarez	–	–	–	–	–
N. setosa s. str.	MNRJP 007644	Brazil, Bahia	12.910°S; 38.497°W	R. Álvarez	OR732508	–	OR732568	Alvarez_NS16	NAI011-23
N. setosa s. str.	MNRJP 007645	Brazil, Bahia	12.910°S; 38.497°W	R. Álvarez	OR732507	OR732536	–	Alvarez_NS17	NAI012-23
N. setosa s. str.	MNRJP 007646	Brazil, Bahia	12.910°S; 38.497°W	R. Álvarez	OR732506	–	OR732567	Alvarez_NS18	NAI013-23
N. setosa s. str.	MNRJP 007647	Brazil, Bahia	12.910°S; 38.497°W	R. Álvarez	OR732505	OR732535	OR732566	Alvarez_NS19	NAI014-23
N. setosa s. str.	MNRJP 007648	Brazil, Bahia	12.910°S; 38.497°W	R. Álvarez	OR732504	OR732534	OR732565	Alvarez_NS20	NAI015-23
N. setosa s. str.	MNRJP 007627	Brazil, Bahia	12.910°S; 38.497°W	R. Álvarez	–	–	–	–	–
N. setosa s. str.	MNRJP 007649	Brazil, Pernambuco	8.355°S; 34.953°W	R. Álvarez	OR732503	OR732533	OR732564	Alvarez_NS21	NAI016-23
N. setosa s. str.	MNRJP 007650	Brazil, Pernambuco	8.355°S; 34.953°W	R. Álvarez	OR732502	OR732532	OR732563	Alvarez_NS22	NAI017-23
N. setosa s. str.	MNRJP 007651	Brazil, Pernambuco	8.355°S; 34.953°W	R. Álvarez	–	OR732531	OR732562	Alvarez_NS23	NAI018-23
N. setosa s. str.	MNRJP 007652	Brazil, Pernambuco	8.355°S; 34.953°W	R. Álvarez	OR732501	OR732530	OR732561	Alvarez_NS24	NAI019-23
N. setosa s. str.	MNRJP 007653	Brazil, Pernambuco	8.355°S; 34.953°W	R. Álvarez	OR732500	OR732529	OR732560	Alvarez_NS25	NAI020-23
N. setosa s. str.	MNRJP 007625	Brazil, Pernambuco	8.355°S; 34.953°W	R. Álvarez	–	–	–	–	–
N. setosa s. str.	ZMBN 157797	Italy, Taranto	40.444°N; 17.241°E	J. Laganeck	OR732499	OR732528	OR732559	Alvarez_NS43	NAI021-23
N. setosa s. str.	ZMBN 157798	Italy, Livorno	43.546°N; 10.302°E	J. Laganeck	OR732498	OR732527	OR732558	Alvarez_NS44	NAI022-23
N. lanai sp. n.	MNRJP 007634	Brazil, Paraná	25.408°S; 48.250°W	R. Álvarez	OR732481	–	OR732543	Alvarez_NS06	NAI023-23

.....*continued on the next page*

TABLE 1. (Continued)

Naineris	Voucher	Site	Coordinates	Collector	COI	16SrRNA	28SrRNA	BOLD Sample ID	BOLD Process ID
N. lanai sp. n.	MNRJP 007635	Brazil, Paraná	25.408°S; 48.250°W	R. Álvarez	OR732482	OR732515	OR732544	Alvarez_NS07	NAI024-23
N. lanai sp. n.	MNRJP 007636	Brazil, Paraná	25.408°S; 48.250°W	R. Álvarez	OR732483	OR732516	OR732545	Alvarez_NS08	NAI025-23
N. lanai sp. n.	MNRJP 007637	Brazil, Paraná	25.408°S; 48.250°W	R. Álvarez	OR732484	OR732517	OR732546	Alvarez_NS09	NAI026-23
N. lanai sp. n.	MNRJP 007638	Brazil, Paraná	25.408°S; 48.250°W	R. Álvarez	OR732488	OR732518	OR732549	Alvarez_NS10	NAI027-23
N. lanai sp. n.	MNRJP 007618	Brazil, Paraná	25.408°S; 48.250°W	R. Álvarez	–	–	–	–	–
N. lanai sp. n.	MNRJP 007619	Brazil, Paraná	25.408°S; 48.250°W	R. Álvarez	–	–	–	–	–
N. lanai sp. n.	MNRJP 007620	Brazil, Paraná	25.408°S; 48.250°W	R. Álvarez	–	–	–	–	–
N. lanai sp. n.	MNRJP 007621	Brazil, Paraná	25.408°S; 48.250°W	R. Álvarez	–	–	–	–	–
N. lanai sp. n.	MNRJP 007622	Brazil, Paraná	25.408°S; 48.250°W	R. Álvarez	–	–	–	–	–
N. lanai sp. n.	MNRJP 007623	Brazil, Paraná	25.408°S; 48.250°W	R. Álvarez	–	–	–	–	–
N. lanai sp. n.	MNRJP 007624	Brazil, Paraná	25.408°S; 48.250°W	R. Álvarez	–	–	–	–	–
N. lanai sp. n.	MNRJP 007654	Brazil, São Paulo	23.815°S; 45.406°W	R. Álvarez	OR732487	–	OR732548	Alvarez_NS28	NAI028-23
N. lanai sp. n.	MNRJP 007655	Brazil, Rio de Janeiro	22.939°S; 43.877°W	J. Gabriel	OR732486	–	OR732547	Alvarez_NS36	NAI029-23
N. lanai sp. n.	MNRJP 007656	Brazil, Rio de Janeiro	22.939°S; 43.877°W	J. Gabriel	OR732485	–		Alvarez_NS38	NAI030-23
Naineris sp.	SERC 252007	USA, California	33.620°N; 117.896°W	E. Keppel	OR732477	OR732511	OR732539	Alvarez_NS46	NAI031-23
Naineris sp.	SERC 252013	USA, California	33.619°N; 117.895°W	E. Keppel	OR732478	OR732512	OR732540	Alvarez_NS47	NAI032-23
Naineris sp.	SERC 251805	USA, California	–	E. Keppel	–	–	–	–	–
Naineris sp.	SERC 251985	USA, California	–	E. Keppel	–	–	–	–	–
Naineris sp.	SERC 252000	USA, California	–	E. Keppel	–	–	–	–	–
Naineris sp.	LACM-AHF Poly	USA, California	32.726°N; 117.192°W	K. Sorensen, C. Sosa	OR732479	OR732513	OR732541	Alvarez_NS33	NAI033-23
Naineris sp.	LACM-AHF Poly	USA, California	32.726°N; 117.192°W	K. Sorensen, C. Sosa	OR732480	OR732514	OR732542	Alvarez_NS34	NAI034-23
Naineris sp.	LACM-AHF Poly	USA, California	32.726°N; 117.192°W	K. Sorensen, C. Sosa	–	OR732510	OR732538	Alvarez_NS35	NAI035-23
N. aurantiaca	MNRJP 007617	Brazil, Santa Catarina	27.783°S; 48.506°W	R. Álvarez	OR795632	OR795716	OR795717	Alvarez_NA01	NAI036-23
N. setosa s. str.	YPM IZ 001242.AN	Bermuda, Flatt's Inlet beach	32.322°N; 64.739°W	–	–	–	–	–	–

.....continued on the next page

TABLE 1. (Continued)

Naineris	Voucher	Site	Coordinates	Collector	COI	16SrRNA	28SrRNA	BOLD Sample ID	BOLD Process ID
N. setosa s. str.	YPM 1303	Bermuda	–	W. R. Coe	–	–	–	–	–
N. setosa s. str.	YPM 1384	Bermuda	–	A. E. Verril	–	–	–	–	–
N. setosa s. str.	AMNH 1972	Bermuda	–	–	–	–	–	–	–
N. setosa s. str.	AMNH 2508A	Bermuda, St. David's Island	–	–	–	–	–	–	–
N. setosa s. str.	USNM 34092	Bermuda	–		–	–	–	–	–
N. setosa s. str.	USNM 181626	Panama, Colon	9.393°N; 79.838°W	STRI	–	–	–	–	–
N. setosa s. str.	USNM 181660	Panama, Colon,	9.395°N; 79.849°W	STRI	–	–	–	–	–
N. setosa s. str.	USNM 174087	Bahamas, San Salvador Island	24.110°N; 74.461°W	R. Zottoli, C. Long	–	–	–	–	–
N. setosa s. str.	USNM 55607	P. Rico, Guanajibo	–	V. Vicente	–	–	–	–	–
N. setosa s. str.	FM 5895	Bahamas, San Salvador Island	24.109°N; 74.462°W	G. Paulay	–	–	–	–	–
N. setosa s. str.	FM 5898	Bahamas, San Salvador Island	24.004°N; 74.476°W	G. Paulay	–	–	–	–	–
N. setosa s. str.	FM 5904	Bahamas, San Salvador Island	24.114°N; 74.462°W	C. Martin	–	–	–	–	–
N. setosa s. str.	FM 5902	Bahamas, San Salvador Island	24.110°N; 74.443°W	C. Martin	–	–	–	–	–
N. setosa s. str.	ColBIO IG 166	–	–	E. F. Nonato	–	–	–	–	–
N. setosa s. str.	ColBIO 168	–	–	E. F. Nonato	–	–	–	–	–
N. setosa s. str.	ColBIO NS20	–	–	E. F. Nonato	–	–	–	–	–
N. cf. *setosa*	AM W.22470	Australia, Sydney	33.873°S; 151.175°E	L. Smith	–	–	–	–	–
N. lanai sp. n.	ZUEC-POL 3784	Brazil, São Paulo	23.623°S; 45.405°W	C. Amaral	–	–	–	–	–
N. lanai sp. n.	ZUEC-POL 3780	Brazil, São Paulo	23.623°S; 45.405°W	C. Amaral	–	–	–	–	–
N. lanai sp. n.	ZUEC-POL 3786	Brazil, São Paulo	23.623°S; 45.405°W	C. Amaral	–	–	–	–	–
N. lanai sp. n.	ZUEC-POL 16999	Brazil, São Paulo	23.747°S; 45.348°W	V. Radashevsky	–	–	–	–	–

.....continued on the next page

TABLE 1. (Continued)

Naineris	Voucher	Site	Coordinates	Collector	COI	16SrRNA	28SrRNA	BOLD Sample ID	BOLD Process ID
N. lanai sp. n.	ZUEC-POL 3771	Brazil, São Paulo	23.627°S; 45.396°W	C. Amaral	–	–	–	–	–
N. lanai sp. n.	ZUEC-POL 2756	Brazil, São Paulo	23.748°S; 45.409°W	C. Amaral	–	–	–	–	–
N. lanai sp. n.	MNRJP 1909	Brazil, Sergipe	11.427°S; 37.335°W	J. Zanol	–	–	–	–	–

TABLE 2. Primers and PCR protocols used in this study.

Marker	Cycle (PCR)					Primer name	Sequence (5'–3')	Direction	Reference
	1x	**5x**			**1x**				
COI	94°C - 40 s	94°C - 40 s	45°C - 40 s	72°C - 120 s	72°C - 7 min	polyLCO	GAYTATWTTCAACAAATCATAAAGATATTGG	Forward	Carr *et al.* (2011)
		40x							
		94°C - 40 s	48°C - 40 s	72°C - 120 s		polyHCO	TAMACTTCWGGGTGACCAAARAATCA	Reverse	Carr *et al.* (2011)
	1x	**40x**			**1x**				
16S	94°C - 3 min	94°C - 30 s	51°C - 30 s (-0.2C per cycle)	72°C - 70 s	72°C - 7 min	16SarL	CGCCTGTTTATCAAAAACAT	Forward	Palumbi *et al.* (1991)
						16SbrH	CCGGTCTGAACTCAGATCACGT	Reverse	Palumbi *et al.* (1991)
	1x	**40x**			**1x**				
16S	94°C - 3 min	94°C - 30 s	52°C - 30 s	72°C - 70 s	72°C - 7 min	AnnF	GCGGTATCCTGACCGTRCWAAGGTA	Forward	Sjölin *et al.* (2005)
						AnnR	TCCTAAGCCAACATCGAGGTGCCAA	Reverse	Sjölin *et al.* (2005)
	1x	**40x**			**1x**				
28S	94°C - 40 s	94°C - 40 s	54°C - 40 s	72°C - 120 s	72°C - 7 min	28v (28gg)	AAGGTAGCCAAATGCCTCGTCATC	Forward	Hillis & Dixon (1991)
						28x (28ii)	GTGAATTCTGCTTCACAATGATAGGAAGAGCC	Reverse	Hillis & Dixon (1991)

Each of the three markers was aligned individually using MAFFT with the automatically chosen L-INSI-i option (Katoh *et al*. 2005). Three markers were concatenated in MegaX (Kumar *et al*. 2018). The phylogenetic analysis was done for individual markers and for the combined partitioned dataset (COI+16S+28S) using Maximum likelihood (ML) implemented in IQ-Tree 2.2.0. (Minh *et al*. 2020) with ultrafast bootstrap (Hoang *et al*. 2018). The substitution models were automatically selected (COI: 1st codon, TNe; 2nd codon, F81+F; 3rd codon, TPM2u+F; 16S: TIM2+F; 28S: TNe+I) (Kalyaanamoorthy *et al*. 2017), and the statistical support of the branches was estimated with 10000 bootstrap replicates. Mean uncorrected pairwise genetic distances (p-distances) for each of the main clades and between the main clades were calculated in MEGA11 (Tamura *et al*. 2021). Haplotype networks of each gene comprising specimens of the *Naineris setosa* complex were built using TCS (Clement *et al*. 2002) in PopART (Leigh & Bryant 2015). The single-marker trees generated in ML analyses were used as the input trees in the species delimitation analyses with Bayesian implementation of the Poisson Tree Processes (bPTP) model (Zhang *et al*. 2013). All analyses were run on the bPTP web server (http://species.h-its.org/) with default settings and pruned outgroups. Final species delimitation hypotheses were formulated based on the combined evidence from morphology and three independent bPTP analyses of individual molecular markers.

Results

Phylogenetic reconstruction

We included 28 specimens of *Naineris* from the coast of Brazil, two specimens from the Mediterranean Sea, and five specimens from the Northeast Pacific. The independent COI, 16S, and 28S alignments were represented by 654, 512, and 626 bases respectively. The concatenated dataset consisted of 1792 bases. The results from the ML analysis are shown in Figure 2.

The combined COI, 16S, and 28S analysis recovered three highly supported clades (BP = 98–100). Phylogenies inferred from the individual markers showed different topologies (Figure 3). A well-supported clade of the Northeastern Pacific specimens was recovered in all analyses and was highly supported (BP = 99, 94, 69; for COI, 16S, and 28S, respectively). In the 16S analysis, only two clades were recovered: all Atlantic specimens formed one clade (BP=100), while the Pacific specimens formed the second clade (BP=94). In the 28S phylogeny, part of the west Atlantic specimens and the specimens from the Mediterranean formed a well-supported clade (BP=88) sister to the Pacific clade (BP=69); however, several specimens from South and Southeastern Brazil were not recovered as a monophyletic group.

Species delimitation analysis resulted in a highly supported delimitation scheme of three putative species based on COI and two putative species based on 16S. The delimitation results of the 28S dataset were generally poorly supported, with the Pacific and one of the Atlantic clades delimited as two putative species and the second Atlantic clade split into six putative species (Fig. 2). Despite several conflicts in delimitation results from three molecular markers, the final species delimitation hypothesis also included information on the morphology and suggested the presence of three species in the dataset: *Naineris setosa* s. str. from the Western Atlantic and the Mediterranean, *Naineris lanai* sp. n. from the South and Southeastern coast of Brazil, and *Naineris* sp. from the Northeastern Pacific.

The TCS haplotype networks (Fig. 4) supported the presence of three species in the COI analysis, with *N. setosa* s. str. having the most frequent haplotype shared among different regions in the Atlantic, including the Mediterranean and the Brazilian coast. *Naineris lanai* sp. n. showed a high diversity of unique haplotypes found in one region – the South and Southeastern Brazilian coast. Two haplotypes of *Naineris* sp. were limited to the Northeastern Pacific locality. The analysis of 16S recovered only two haplotypes in the whole dataset; one shared among all the Atlantic specimens, including both *N. setosa* s. str. and *N. lanai* sp. n., and the second haplotype reported in the Pacific. In the 28S analysis, all *N. setosa* s. str. shared a single haplotype reported in the Eastern and the Western Atlantic. The unidentified species from the Northeastern Pacific and *N. lanai* sp. n. showed the presence of two haplotypes in 28S.

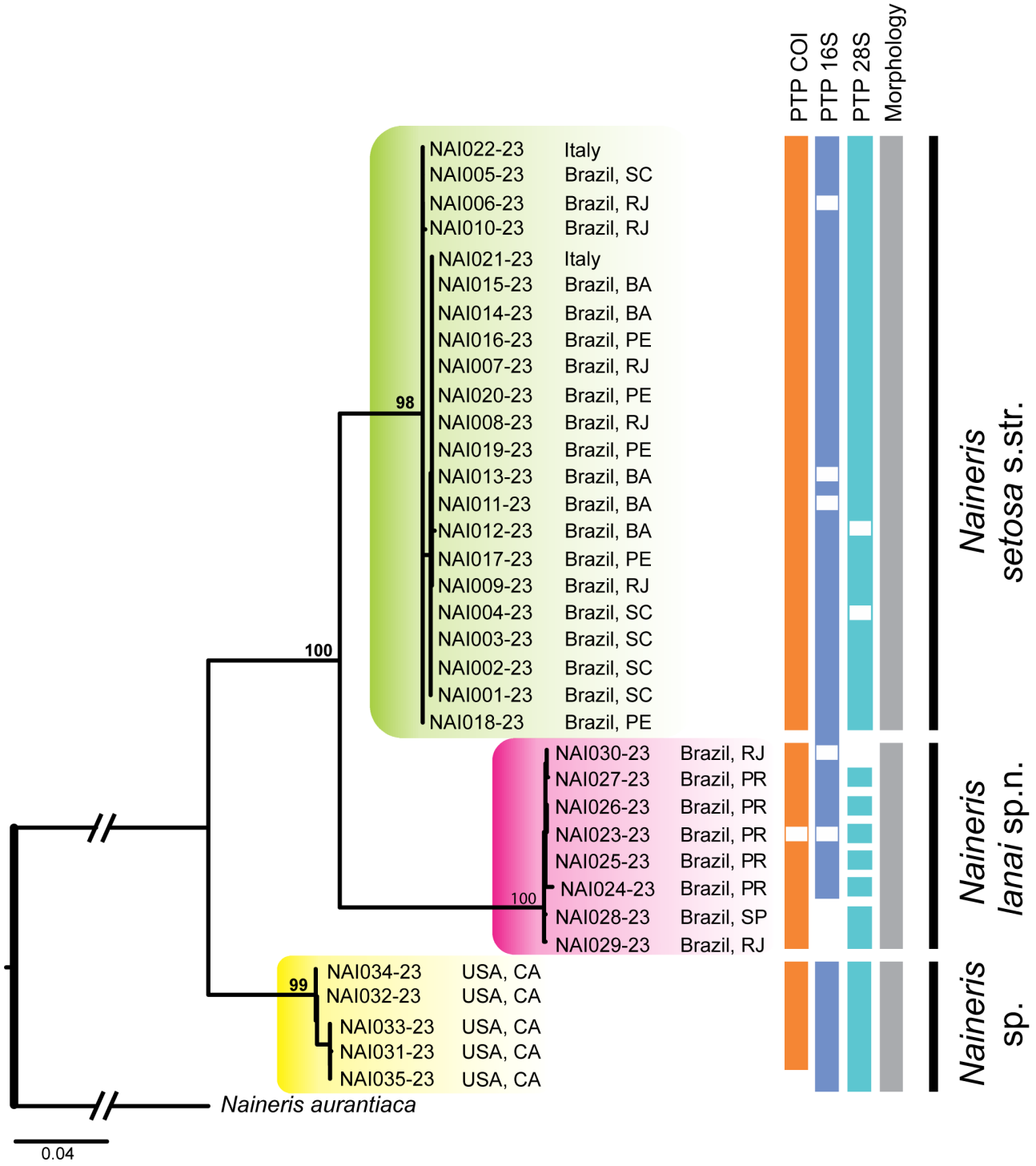

FIGURE 2. Maximum Likelihood tree of the combined COI, 16S, and 28S dataset; numbers on nodes indicate ultrafast bootstrap support values; species delimitation results inferred by morphology and DNA-based methods are indicated right to the consensus tree; bPTP was applied separately to the individual gene trees. White bars indicate missing data.

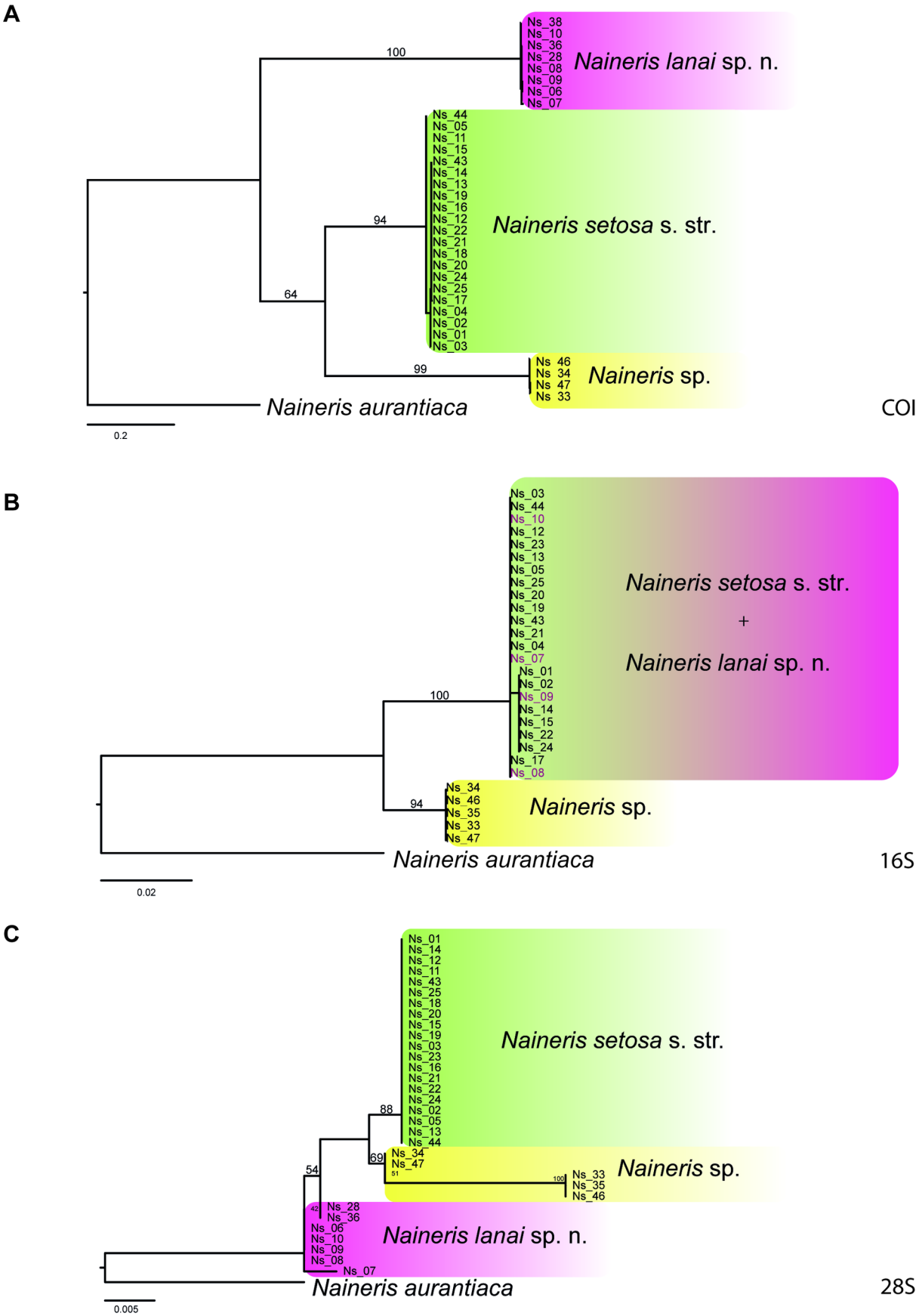

FIGURE 3. Maximum Likelihood trees of single COI, 16S, and 28S markers; numbers on nodes indicate ultrafast bootstrap support values.

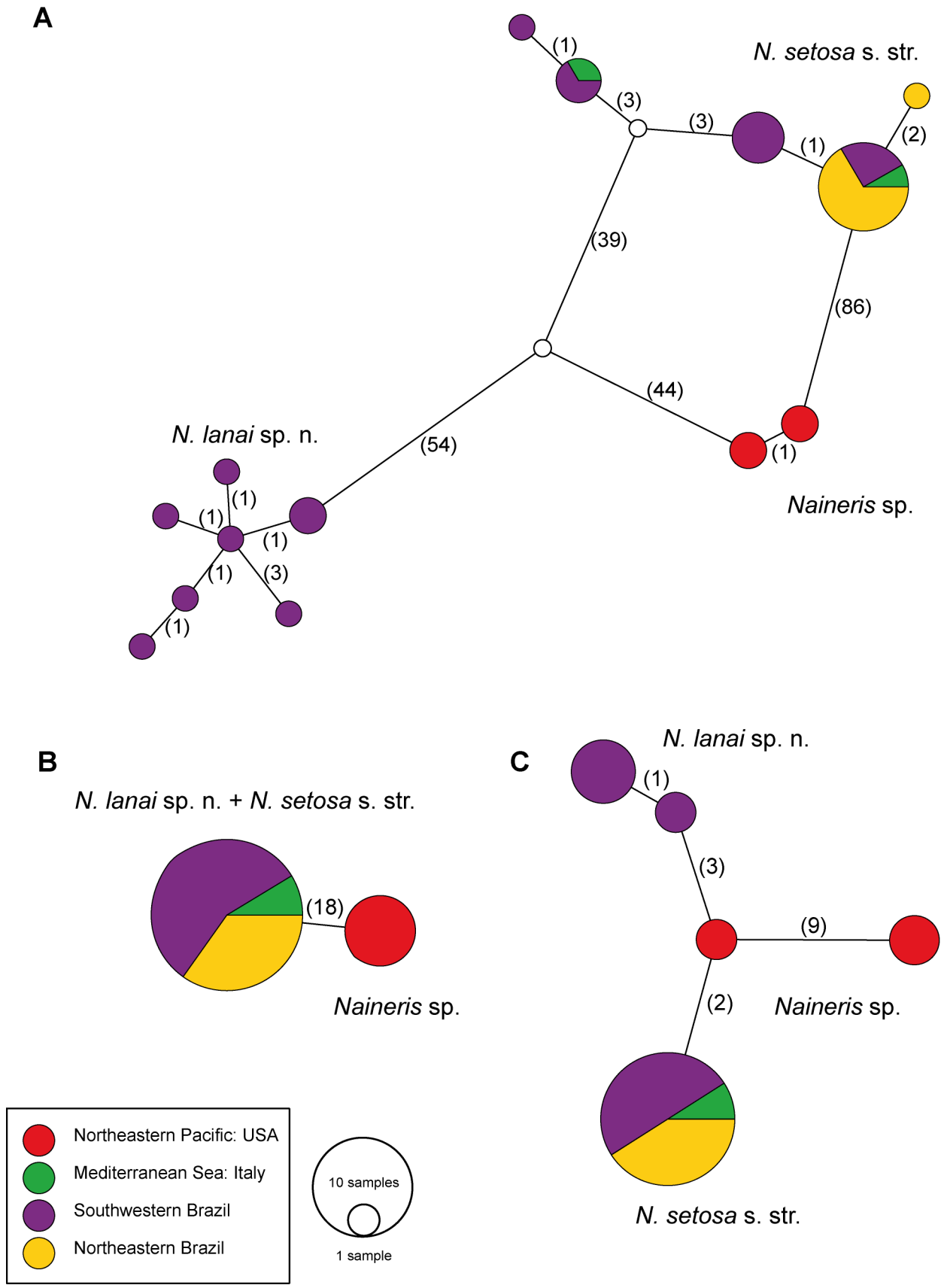

FIGURE 4. Haplotype networks of the *Naineris setosa* species complex based on COI (A), 16S (B), and 28S (C). Colors correspond to geographic areas. Circle sizes correspond to sample size. Numbers in parentheses show the number of substitutions between the haplotypes.

Genetic distances

The genetic distances are summarized in Tables 3–6. The estimated genetic divergences between the three clades in COI ranged from 13.7 to 16%, in 16S from 0 to 6.1%, and in 28S from 1.1 to 1.8%. The intraspecific genetic divergences in COI were 0.1–0.4% and in 28S 0–1.1%. There was no intraspecific divergence in 16S.

TABLE 3. Percentage of uncorrected p-distance matrix within clades of the *Naineris setosa* species complex based on COI, 16S, and 28S DNA sequences.

Naineris	**COI**	**16S**	**28S**
Naineris sp.	0.001	0.000	0.011
N. setosa s. str.	0.004	0.000	0.000
N. lanai sp. nov.	0.004	0.000	0.001

TABLE 4. Percentage of uncorrected p-distance matrix between clades of the *Naineris setosa* species complex based on COI sequences.

Naineris	*Naineris* sp.	*N. setosa* s. str.	*N. lanai* sp. nov.
Naineris sp.	-		
N. setosa s. str.	0.137	-	
N. lanai sp. nov.	0.160	0.155	-

TABLE 5. Percentage of uncorrected p-distance matrix between clades of the *Naineris setosa* species complex based on 16S sequences.

Naineris	*Naineris* sp.	*N. setosa* s. str.	*N. lanai* sp. nov.
Naineris sp.	-		
N. setosa s. str.	0.061	-	
N. lanai sp. nov.	0.061	0	-

TABLE 6. Percentage of uncorrected p-distance matrix between clades of the *Naineris setosa* species complex based on 28S sequences.

Naineris	*Naineris* sp.	*N. setosa* s. str.	*N. lanai* sp. nov.
Naineris sp.	-		
N. setosa s. str.	0.015	-	
N. lanai sp. nov.	0.018	0.011	-

Taxonomic account

Family ORBINIIDAE Hartman, 1942

Genus *Naineris* Blainville, 1828

Type species. *Naineris quadricuspida* (Fabricius, 1780)

Diagnosis (amended from Blake 2020; Zhadan 2020). Prostomium rounded, truncated, or weakly bifid on anterior margin. Peristomium with one or two achaetous rings. Thorax with 12–30 or more segments; branchiae first present from chaetigers 2–23. Thoracic neuropodia with 0–2 postchaetal lobes; no subpodial lobes. Thoracic neurochaetae include capillaries, or capillaries mixed with blunt-tipped uncini, sometimes hooded, or uncini and subuluncini. Abdominal chaetae include capillaries, sometimes furcate chaetae in notopodia, and capillaries and embedded or protruding aciculae in neuropodia. Dorsal sensory organs present in some species, being paired or multiple, rounded or as elongated semicircles. Dorsal cilia within branchiae bases present, either forming flat bands or crests.

***Naineris setosa* (Verril, 1900) s. str.**
(Figs 5–8)

Aricia setosa Verrill, 1900: 651–653.
Anthostoma latacapitata Treadwell, 1901: 203–204, figs 61–65.
Nainereis latacapitata: Treadwell 1939: 264, fig. 81.
Naineris setosa: Treadwell 1936: 55; Hartman 1957: 305, pl. 41, figs 1–6 (in part); Nonato 1981: 149–150, figs 177–179; Solis-Weiss & Fauchald 1989: 774–778, figs 2a–j; Blake & Giangrande 2011: 20–26, figs 1–2; Khedhri *et al*. 2014: 83–88, fig. 2; Atzori *et al*. 2016: 1–6.

Material examined. Atlantic Ocean. Bermuda: YPM 001242.AN (lectotype), YPM 1303 (1 spm), YPM 1384 (1 spm), USNM 34092 (1 spm), AMNH 1972 (4 spms), AMNH 2508A (2 spms). **Panama, Caribbean Sea**: USNM 181626 (1 spm), USNM 181660 (1 spm). **Puerto Rico**: USNM 55607 (19 spms). **Bahamas. San Salvador Island, Oyster Pond:** FM 5895 (1 spm), USNM 174087 (10 spms), **Pigeon Creek Mangrove:** FM 5898 (1 spm), **Moon Rock Pond**: FM 5904 (1 spm), **Crescent Pond**, FM 5902 (2 spms). **Brazil. Pernambuco, Cabo de Santo Agostino:** MNRJP 007649 (DNA voucher Ns21), MNRJP 007650 (DNA voucher Ns22), MNRJP 007651 (DNA voucher Ns23), MNRJP 007652 (DNA voucher Ns24), MNRJP 007653 (DNA voucher Ns25), MNRJP 007625 (5 spms). **Rio de Janeiro, Cabo Frio**: MNRJP 007639 (DNA voucher Ns11), MNRJP 007640 (DNA voucher Ns12), MNRJP 007641 (DNA voucher Ns13), MNRJP 007642 (DNA voucher Ns14), MNRJP 007643 (DNA voucher Ns15), MNRJP 007626 (13 spms), **Ilha Grande**: ColBIO IG 166 (1 spm), ColBIO IG 168 (2 spms), ColBIO NS20 (7 spms). **Santa Catarina, Santa Catarina Island**: MNRJP 007629 (DNA voucher Ns1), MNRJP 007630 (DNA voucher Ns2), MNRJP 007631 (DNA voucher Ns3), MNRJP 007632 (DNA voucher Ns4), MNRJP 007633 (DNA voucher Ns5), MNRJP 007628 (4 spms). **Bahia, Salvador**: MNRJP 007644 (DNA voucher Ns16), MNRJP 007645 (DNA voucher Ns17), MNRJP 007646 (DNA voucher Ns18), MNRJP 007647 (DNA voucher Ns19), MNRJP 007648 (DNA voucher Ns20), MNRJP 007627 (8 spms). **Italy. Taranto:** ZMBN 157797 (DNA voucher Ns43). Livorno: ZMBN 157798 (DNA voucher Ns44). **Australia. Rozelle Bay, Sydney:** AM W.22470 (4 spms).

Type locality. Flatt's Inlet Beach, Bermuda. Shell-sand, low intertidal.

Diagnosis. Thoracic neurochaetae only crenulated capillaries, thoracic segments without ventral groove and notches, paired dorsal sensory organs present, low dorsal crest from abdominal segments, thoracic neuropodial lobe with upper papilla, as wide flanges with well-delimited boundaries.

Description (based on the lectotype). Lectotype (YPM IZ 001242.AN) incomplete, 149 chaetigers, 57 mm long, 0.7 mm wide at chaetiger 50. Color in alcohol light tan (live Brazilian specimens pale yellow with reddish branchiae, bearing long fluorescent cilia along branchial axis and between them). Thorax and abdomen marked by dorsal displacement of parapodia in abdomen (Figs 5A; 7A). Ventral surface smooth, ventral groove only present in abdominal segments (Fig. 8A, B), ventral notches absent.

Prostomium wider than long, more or less square and rounded in front and corners (Figs 5B; 7A); eyespots along lateral margins; nuchal organs discernible (Fig. 7A, B). Peristomium with two annular rings, only weakly marked; mouth opening situated ventrally and surrounded by striated lips; proboscis, not everted, presumably broad and lobed as in topotype specimens.

Branchiae first present from chaetiger 5–6, cirriform, tapering to sharp tip, with dense cilia, first branchiae long, reaching ⅓ of abdominal branchiae (Fig. 5B). Conspicuous dorsal sensory organs from chaetiger 7, oval-shaped and paired, with dense cilia (Fig. 7C). Dorsal crest present from abdominal segments; straight, supported by thick base; low, approximately ¼ diameter of branchiae, ciliated.

Thorax comprises 20 chaetigers, moderately flattened (Fig. 5A). Parapodia biramous; interramal papilla absent. Notopodial lobes lanceolate. Neuropodial lobes represented by wide flanges ending above digitate papillae, with well-delimited boundaries (Figs 5A, C; 6A). Abdominal notopodial and neuropodial lobes cirriform (Figs 5D; 6B); abdominal notopodial lobes longer or equal to thoracic notopodial lobes, shorter than branchiae (Figs 5D; 6B).

Thoracic notochaetae with two bundles of about 20–30 crenulated capillaries at different levels (Figs 5C; 6A). Abdominal notochaetae arranged in two groups of 10–15 crenulated capillaries and furcate chaetae (Figs 6B; 7F); furcate chaetae with unequal tines and tiny needles at different levels (Fig. 7F), placed in a lower position, difficult to observe; shaft bearing numerous crowded transversal rows of about 10–12 small barbs (Fig. 7F). Thoracic neurochaetae with around seven rows of numerous capillaries (Figs 5C; 6A, E) separated into two groups by oblique gap (Fig. 5C). Abdominal neurochaetae with 5–10 capillaries and three acicular spines (Figs 6B; 7D). Pygidium missing.

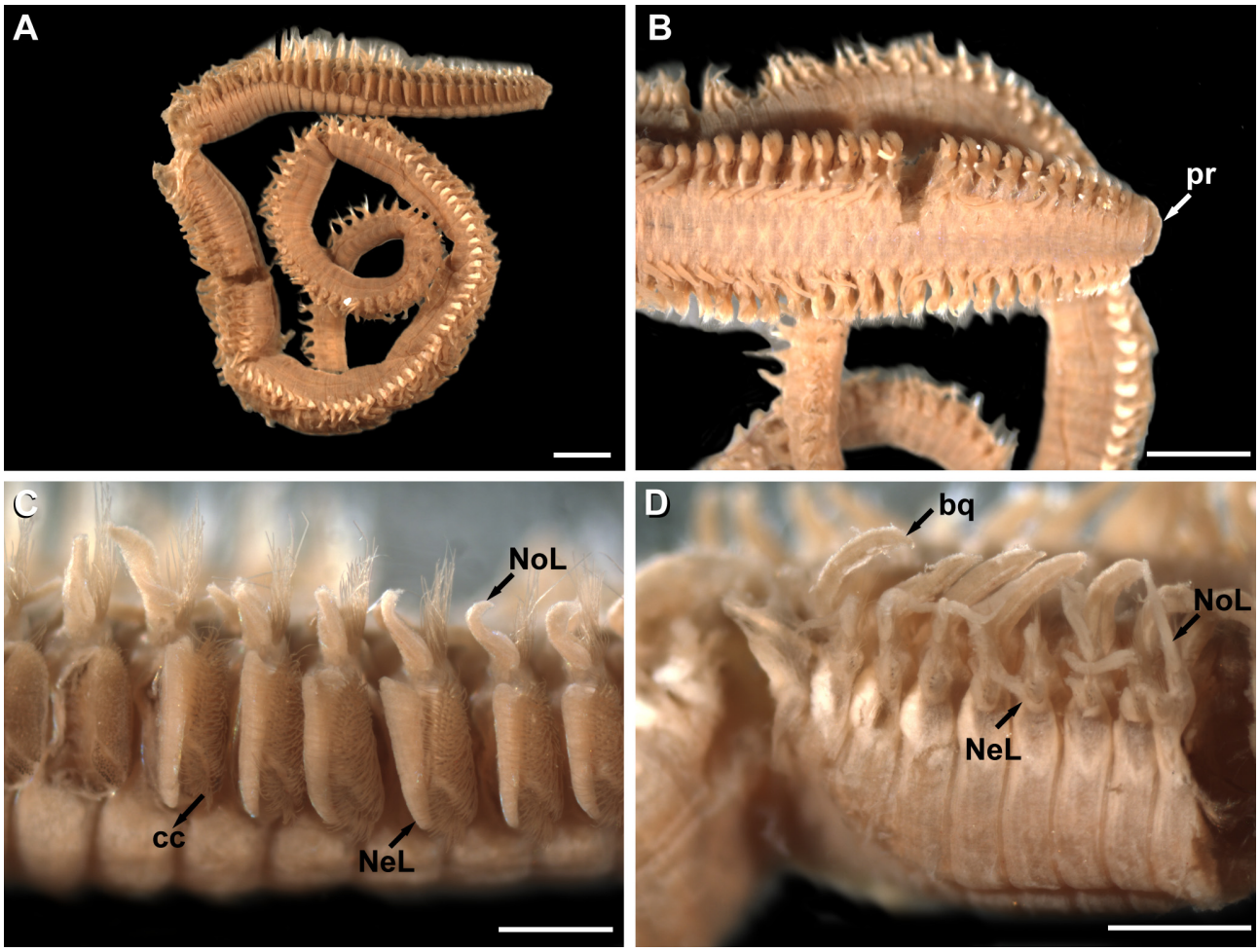

FIGURE 5. *Naineris setosa*, lectotype (YPM IZ 001242.AN): (A) Lateral view; (B) Anterior end, dorsal view; (C) Thoracic parapodia; (D) Abdominal parapodia. bq—branchia, cc—crenulate capillaries, NeL—neuropodial lobe, NoL—notopodial lobe, pr—prostomium. Scale bars; (A–B): 0.7 mm; (C–D): 0.35 mm.

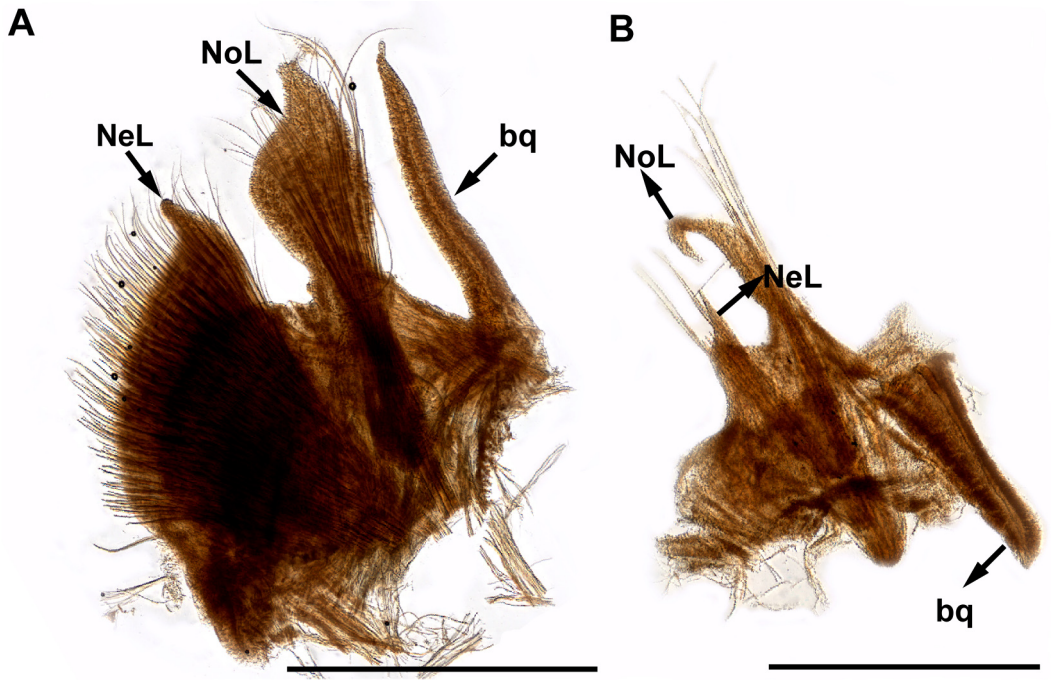

FIGURE 6. *Naineris setosa*, lectotype (YPM IZ 001242.AN): (A) Thoracic parapodium (ch. 11); (B) Abdominal parapodium (ch. 91). bq—branchia (displaced), NeL—neuropodial lobe, NoL—notopodial lobe. Scale bars; (A–B): 1 mm.

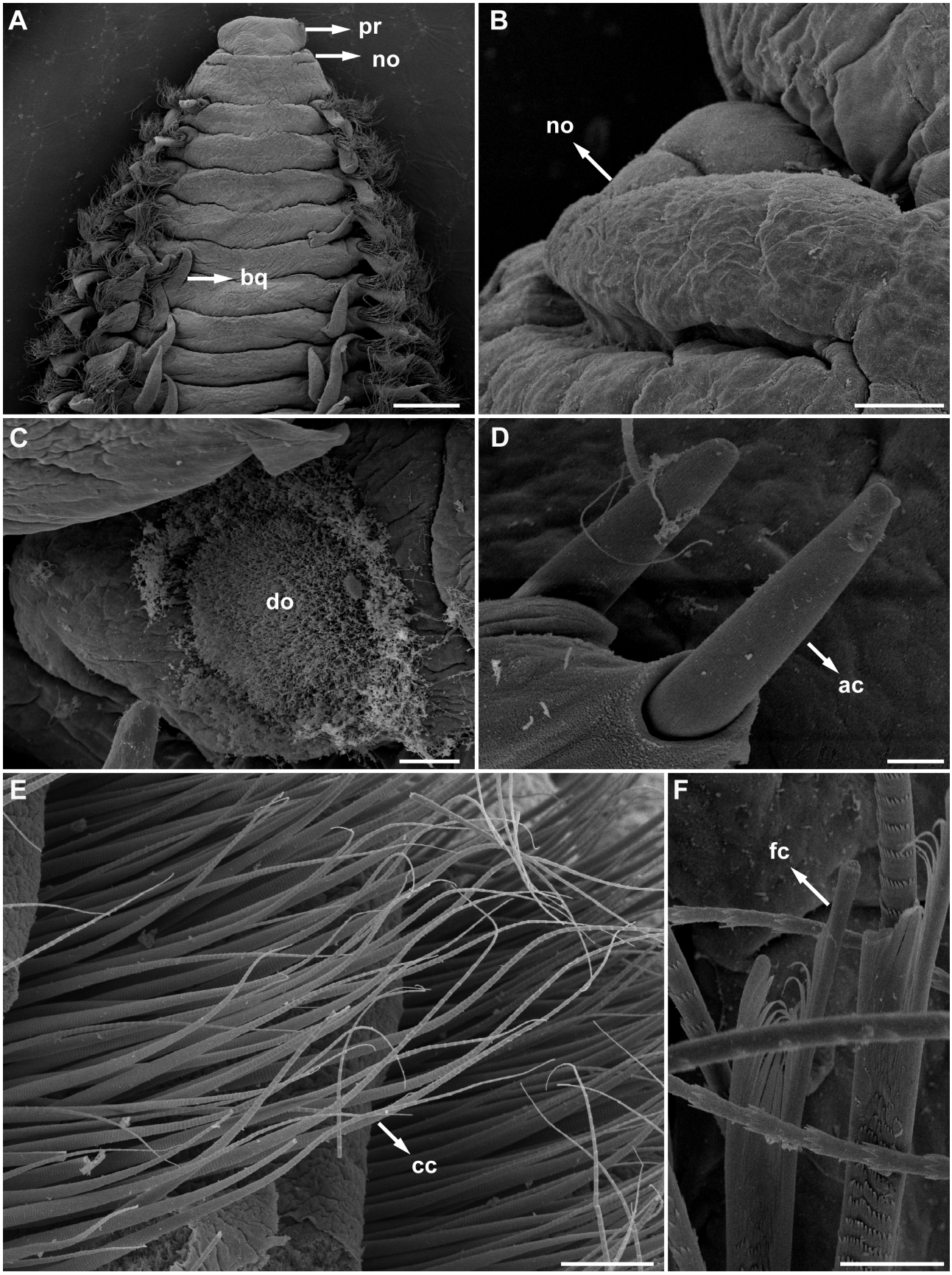
A
pr
no
bq
B
no
C
do
D
ac
E
cc
F
fc

FIGURE 7. *Naineris setosa* from Pernambuco, Brazil (MNRJP 007720) examined under SEM: (A) Anterior end, dorsal view; (B) Nuchal organ; (C) Dorsal organ; (D) Acicular spines; (F) Furcate chaetae. *Naineris setosa* from Bahamas under SEM (FM 5898): (E) Thoracic neurochaetae. ac—acicular spines, bq—branchia, cc—crenulated capillaries, do—dorsal organ, fc—furcate chaeta, no—nuchal organ, pr—prostomium. Scale bars; (A): 500 μm; (B): 50 μm; (C): 20 μm; (D): 5 μm; (E–F): 10 μm.

Remarks. Hartman (1951) examined specimens from the Gulf of Mexico and synonymized *Anthostoma lacapitata* Treadwell, 1901 with *Naineris setosa*. Solis-Weiss & Fauchald (1989) redescribed the syntype of *N. setosa* retaining its wide distribution in the tropical Northwest Atlantic, herein designated as the lectotype (ICZN 1999, Art. 74). Subsequently, Blake & Giangrande (2011) reported the species as invasive in the Mediterranean Sea. The species was also reported from the Adriatic and the Tyrrhenian Seas expanding its distribution to Tunisia and Taranto (Arduini *et al*. 2022, Rebai *et al*. 2022). The records from the Pacific, such as those from Galapagos and Australia, require further revision. We examined the specimen from Galapagos studied by Blake, but it was in poor condition preventing accurate identification.

Pygidium was not observed in the lectotype, but in the examined Brazilian specimens it agreed with Solís-Weiss & Fauchald's (1989) description, stating that *N. setosa* bears four anal cirri. Morphological variation of Brazilian populations of *N. setosa* s. str. is shown in Table 7.

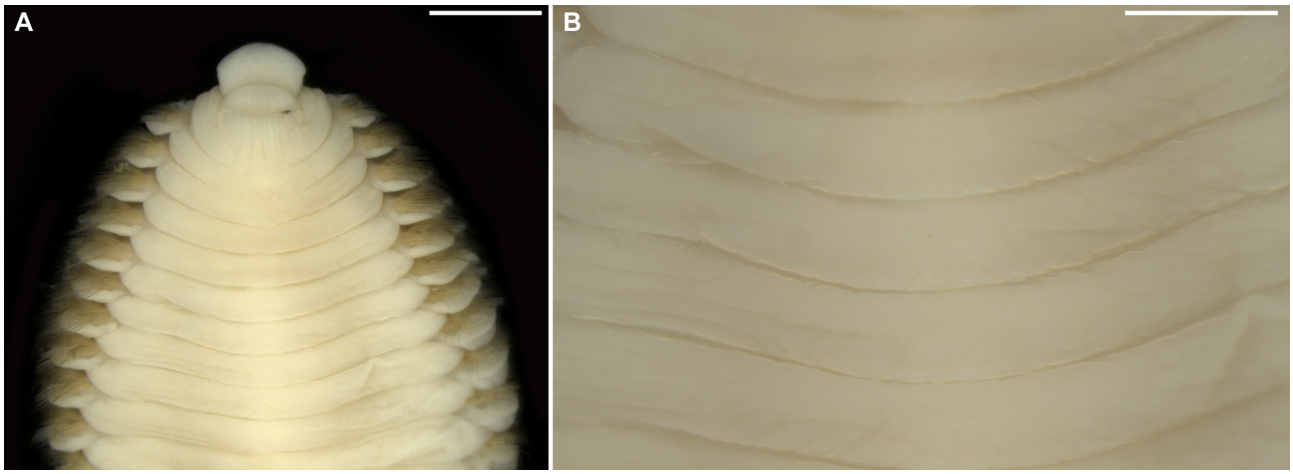

FIGURE 8. *Naineris setosa* from Taranto, Mediterranean Sea (ZMBN 157797): (A) Anterior end, ventral view; (B) Smooth, thoracic ventral surface. Scale bars; (A): 1 mm; (B): 500 μm.

Habitat. Shell-sand, intertidal.

Distribution. Intertidal and shallow subtidal (down to 1 m deep) zone of the Atlantic. Western Atlantic: Bermuda, Bahamas, Gulf of Mexico, Caribbean Sea, Panamá, Belize, Puerto Rico, and Brazilian coast. Presumably invasive in the Mediterranean Sea (Blake & Giangrande 2011; Khedhri *et al*. 2014; Dean & Blake 2015; Atzori *et al*. 2016).

Naineris lanai sp. n.

(Figs 9–11)

Material examined. Brazil. Paraná, Pinheiros Bay: MNRJP 007618 (holotype), MNRJP 007619 (2 paratypes), MNRJP 007624 (1 paratype), MNRJP 007622 (7 paratypes), MNRJP 007621 (10 paratypes), MNRJP 007634 (paratype, DNA voucher Ns06), MNRJP 007635 (paratype, DNA voucher Ns07), MNRJP 007636 (paratype, DNA voucher Ns08), MNRJP 007637 (paratype, DNA voucher Ns09), MNRJP 007638 (paratype, DNA voucher Ns10), MNRJP 007620 (6 paratypes), **Paranaguá Bay**: MNRJP 007623 (2 paratypes). **Rio de Janeiro, Itacuruçá:** MNRJP 007655 (paratype, DNA voucher Ns36), MNRJP 007656 (paratype, DNA voucher Ns38). **São Paulo, Araçá:** MNRJP 007654 (paratype, DNA voucher Ns28), **Ilhabela**, ZUEC-POL 16999 (2 spms), ZUEC-POL 2756 (1 spm), **Caraguatatuba**, ZUEC-POL 3780 (1 spm), ZUEC-POL 3784 (1 spm), ZUEC-POL 3786 (1 spm), ZUEC-POL 3771 (1 spm). **Sergipe. Praia do Saco:** MNRJP 1909 (1 spm).

TABLE 7. Measurements and morphological variation in different populations of *Naineris setosa* s. str. and *Naineris lanai* sp. n. from its type locality (Means+/-standard deviation (minimum-maximum)). Th. ch.—thoracic chaetigers, Width—width at chaetiger 50, Bq. start—chaetiger where branchiae first appear, Bq. length—branchial length at chaetiger 50, DO start—chaetiger where dorsal organs first appear, DC length—dorsal crest length at chaetiger 50, NoL—Notopodial lobe length at chaetiger 50, NeL—Neuropodial lobe length at chaetiger 50.

Species	Locality	Th. ch.	Width (mm)	Bq. start	Bq. length (mm)	DO start	DC length (mm)	NoL length (mm)	NeL length (mm)
N. setosa s. str.	Pernambuco	22.2+/-1.03 (21–24)	1.78+/-0.3 (1.4–2.2)	6+/-0 (6–6)	1.0+/-0.16 (0.7–1.2)	8.7+/-0.82 (8–10)	0.16+/-0.04 (0.1–0.2)	0.76+/-0.13 (0.6–1.0)	0.29+/-0.07 (0.2–0.4)
N. setosa s. str.	Bahia	22.4+/-0.96 (21–24)	2.33+/-0.45 (2.0–3.4)	6+/-0 (6–6)	1.36+/-0.16 (1.1–1.5)	8.7+/-0.82 (8–10)	0.15+/-0.03 (0.1–0.2)	0.83+/-0.13 (0.7–1.1)	0.41+/-0.07 (0.3–0.5)
N. setosa s. str.	Cabo Frio	23.5+/-1.35 (21–25)	2.25+/-0.29 (1.6–2.6)	6+/-0 (6–6)	1.28+/-0.3 (0.8–1.6)	8.9+/-1.1 (7–11)	0.15+/-0.07 (0.05–0.25)	0.78+/-0.15 (0.6–1.1)	0.38+/-0.08 (0.3–0.5)
N. setosa s. str.	Santa Catarina	20.1+/-1.45 (18–23)	1.26+/-0.33 (0.7–1.8)	6+/-0 (6–6)	0.9+/-0.12 (0.7–1.1)	8.1+/-1.28 (7–10)	0.11+/-0.02 (0.1–0.15)	0.68+/-0.17 (0.5–1.1)	0.27+/-0.06 (0.2–0.35)
N. lanai sp. n.	Paraná	29.4+/-1.07 (27–30)	3.79+/-0.69 (3.0–5.1)	6+/-0 (6–6)	2.35+/-0.24 (2.1–2.75)	9.2+/-0.91 (8.8–11)	0.45+/-0.05 (0.4–0.55)	1.42+/-0.28 (0.8–1.8)	0.55+/-0.13 (0.3–0.7)

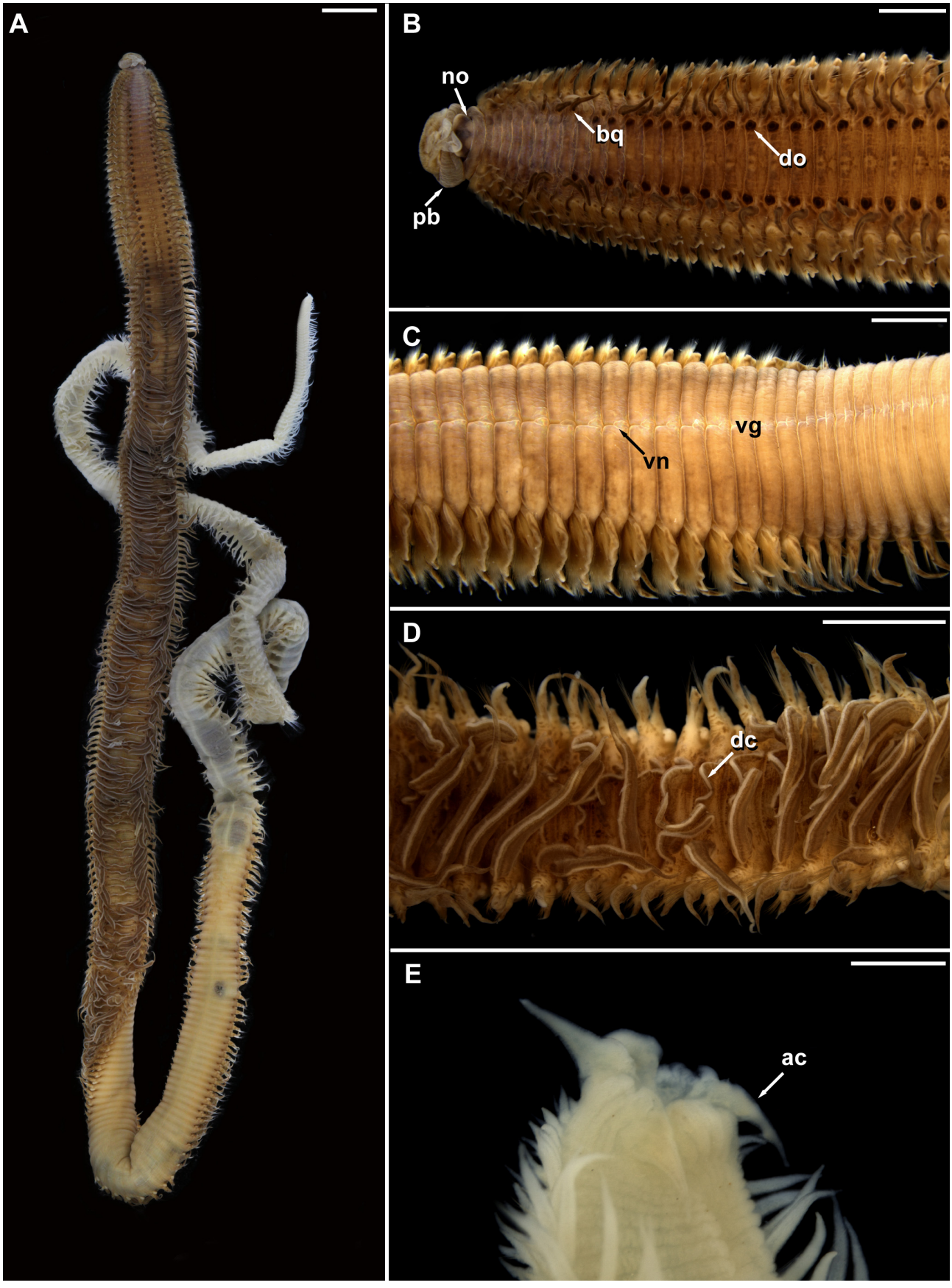
A
B
no
bq
do
pb
C
vg
vn
D
dc
E
ac

FIGURE 9. *Naineris lanai* sp. n., holotype (MNRJP 007618): (A) Complete specimen, dorsal view; (B) Anterior end, dorsal view; (C) Thoracic segments, ventrolateral view; (D) Abdominal segments, dorsal view; (E) Posterior end, dorsolateral view. ac—anal cirrus, bq—branchiae, dc—dorsal crest, do—dorsal organs, no—nuchal organ, pb—proboscis, vg—ventral groove, vn—ventral notches. Scale bars; (A): 5 mm; (B–D): 2 mm; (E): 500 μm.

Type locality: Brazil: Paraná (Pinheiros Bay), 25.409° S, 48.251° W, intertidal, 20 cm depth, anoxic mud, close to *Spartina* sp.

Etymology. *Naineris lanai* is named in honor of R.A.'s late Ph.D. supervisor, the Brazilian scientist Paulo da Cunha Lana, in recognition of his substantial contribution to marine science and for believing in people.

Diagnosis. Thoracic neurochaetae including crenulated capillaries only; thoracic segments with ventral groove and notches; paired dorsal sensory organs present; ciliary dorsal crest in abdominal segments folded and hypertrophied; thoracic neuropodial lobes flattened and folded with irregular boundaries, with upper papilla; notopodial lobes undivided or forked.

Description. Large species (Figs 9A; 11E), holotype complete (MNRJP 007618), 263 mm long, 5 mm wide, consisting of 431 chaetigers. Color in alcohol dark brown, with dark segmental spots; live specimens dark brown to reddish, with dark pigmented branchiae and dorsal organs, and long fluorescent cilia along axis; eyespots and nuchal organs yellowish, dorsal crest bearing long fluorescent cilia. Body separated into two distinct regions of approximately same width (Fig. 9A); thorax and abdomen, with parapodia displaced dorsally in abdomen. Ventral surface of body rough, with prominent mid-ventral groove along most of body (Figs 9C; 11C), well-marked in thoracic segments, represented by longitudinal notch on each segment, almost reaching consecutive ring (Fig. 9C).

Prostomium wide, nearly square, spatulate in front (Fig. 9B); eyespots present on lateral margins of prostomium, organized in two groups; nuchal organs present, as two lateral notches between prostomium and peristomium (Fig. 9B), more conspicuous and globular in live specimens (Fig. 11A). Peristomium as single achaetous ring; mouth opening located ventrally; proboscis wide, thick, bearing triangular lobes (Figs 9B; 11A, B), densely ciliated (Fig. 10A).

Branchiae from chaetigers 5–6, continuing along entire body (Fig. 9A, B); elongate from first pair, widest basally, tapering to narrow apex, with medial and lateral cilia. Thoracic branchiae ⅓ of longest abdominal branchiae. Paired dorsal sensory organs from mid-thoracic chaetigers, anterior and medial to branchial bases, oval-shaped, clearly raised (Figs 9B; 10B). Dorsal crest present in abdominal segments; straight at first, best developed and more extended in mid-abdominal segments becoming folded, as long as or even exceeding basal width of branchiae (Figs 9A, D; 10D).

Thorax with 30 chaetigers (28–30 in paratypes), flattened. Parapodia biramous; interramal papilla absent. Thoracic notopodia with lanceolate lobes, more elongate in posterior chaetigers; forked or undivided. Neuropodial lobes wide, flat, with rough flanges with irregular borders, almost folded (Fig. 9C). Abdominal notopodial and neuropodial lobes similar in shape, triangular to lanceolate, with thin apex; notopodial lobes more prolonged than neuropodial lobes (Fig. 11D).

Thoracic notochaetae with two bundles of around 30–50 crenulated capillaries. Abdominal notochaetae with 15–20 crenulated capillaries in two bundles and furcate chaetae in lower position (Fig. 10C); each furcate chaeta with unequal tines, bearing tiny needles; shaft with small barbs. Thoracic neurochaetae with about 7–9 rows of capillaries separated into two groups by oblique gap. Abdominal neurochaetae with 15–20 capillaries and 2–3 acicular spines.

Pygidium with terminal anus, bearing four anal cirri with forked or undivided tips, and rounded bases (Fig. 9E).

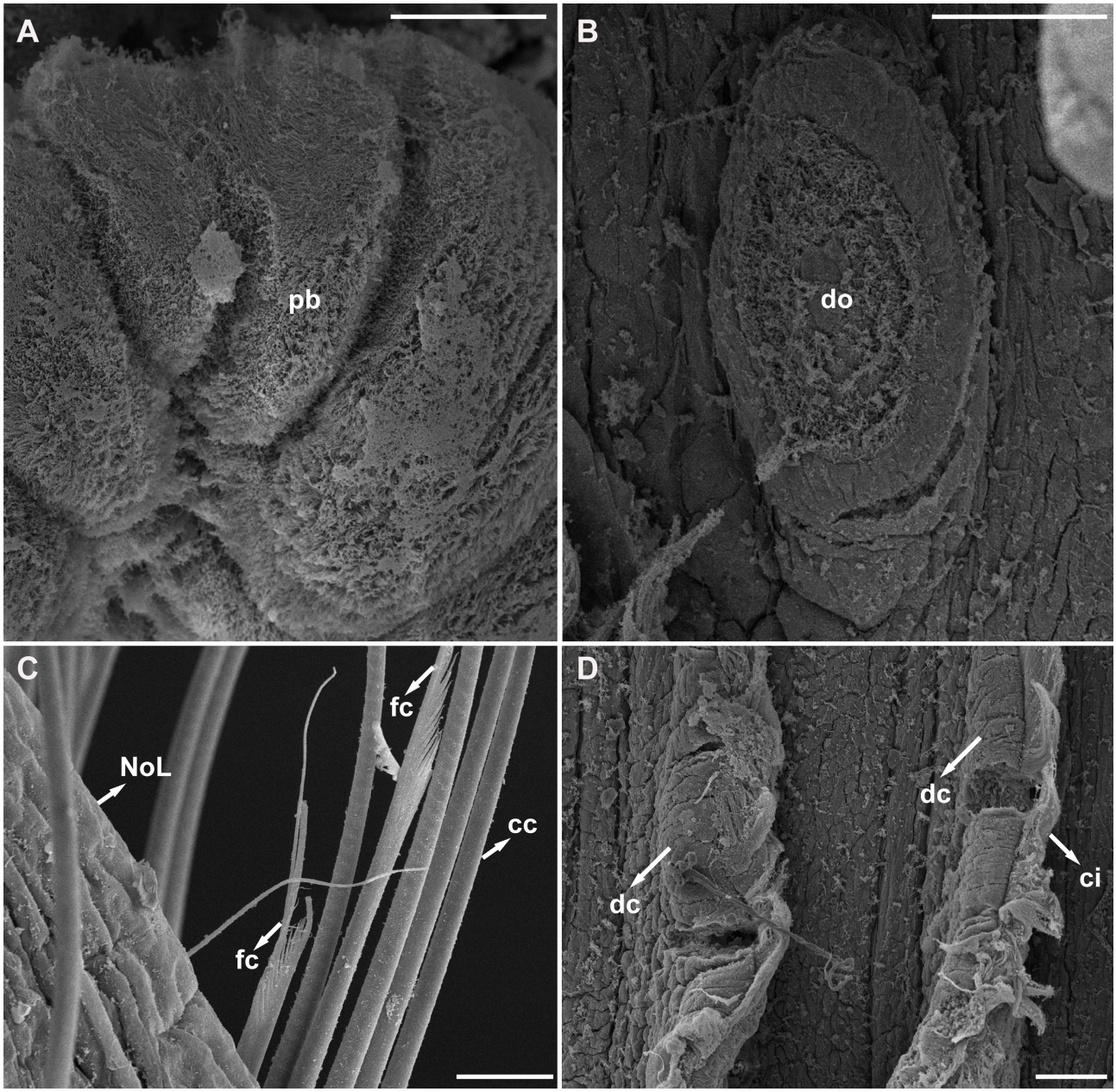

FIGURE 10. *Naineris lanai* sp. n. topotype specimen examined under SEM, A–B, MNRJP 007721; C–D, MNRJP 007722: (A) Cilia in the everted proboscis, ventral view; (B) Dorsal organ in thoracic segment; (C) Furcate chaetae in abdominal segment, lateral view; (D) Cilia in dorsal crest. cc—crenulated capillaries, ci—cilia, dc—dorsal crest, do—dorsal organ, fc—furcate chaetae, pb—proboscis, NoL—notopodial lobe. Scale bars; (A): 50 mm; (B): 500 µm; (C): 20 µm; (D): 100 µm.


A
e
no
B
pb
bq
do
C
vn
vn
D
E
F
G
H
I

FIGURE 11. Habitat (H) and live (A–D, I) and preserved (E–G; paratype MRNJP 007623) specimens of *Naineris lanai* sp. n.: (A) Anterior end with a partially everted proboscis, dorsal view; (B) Anterior end with a completely everted proboscis, dorsal view; (C) Thoracic segments, ventral view; (D) Abdominal segments, lateral view; (E–G) Furcation in abdominal notopodial lobes; (H) Tidal flat from Ilha das Peças, Pinheiros Bay, the type locality; (I) Specimens being sorted in the laboratory. bq—branchia, do—dorsal organ, e—eyespots, no—nuchal organ, pb—proboscis, vn—ventral notch (Arrows point to furcate notopodial lobes). Scale bars; (A): 0.5 mm; (B): 2 mm; (C): 0.2 mm; (D): 1 mm; (E-G): 0.1 mm.

Remarks. *Naineris lanai* sp. n. is similar to *N. setosa* s. str. in having only crenulated capillaries in thoracic neuropodia, dorsal crest, and branchiae from chaetigers 5–6. It differs from *N. setosa* in the dorsal crest being long and folded, and having marked ventral groove in thoracic segments, flat and folded thoracic neuropodial lobes, and often divided abdominal notopodial lobes.

Considering the anoxic habitat of the species, the hypertrophied ciliary dorsal crest, and parapodial lobes, are probably an adaptation to this environment. Similar correlation was established for some species of Nereididae and Opheliidae living in anoxic conditions (Glasby *et al*. 2021). The shape of thoracic neuropodial lobes differs significantly in both species. In *Naineris setosa* s. str., neuropodial lobes are thick, elongated processes with rounded boundaries. In *N. lanai* sp. n., neuropodial lobes are enlarged, markedly flat, and folded with irregular boundaries. This may also be an adaptation to increase the surface area for oxygen uptake, such as in other polychaetes (Hartman 1951; Nonato *et al*. 1986; Radashevsky & Lana 2009; Glasby *et al*. 2021).

Habitat. Large mature adults were sampled in black anoxic mud near *Spartina* sp. and mangroves from Pinheiros Bay, Paranaguá Estuarine Complex (Fig. 11E). Juveniles were sampled in mud from São Paulo and fouling communities from Rio de Janeiro.

Distribution. South and Southeastern Brazil, from Paraná to Rio de Janeiro, intertidal.

Naineris sp.

(Fig. 12)

Material examined. USA, California. SERC 252007 (DNA voucher Ns46, + 1 spm), SERC 252013 (DNA voucher Ns47, + 2 spms), SERC 251805 (1 spm), SERC 251985 (1 spm, 1 for SEM), SERC 252000 (2 spms), LACM-AHF: DNA vouchers Ns33, Ns34, Ns35.

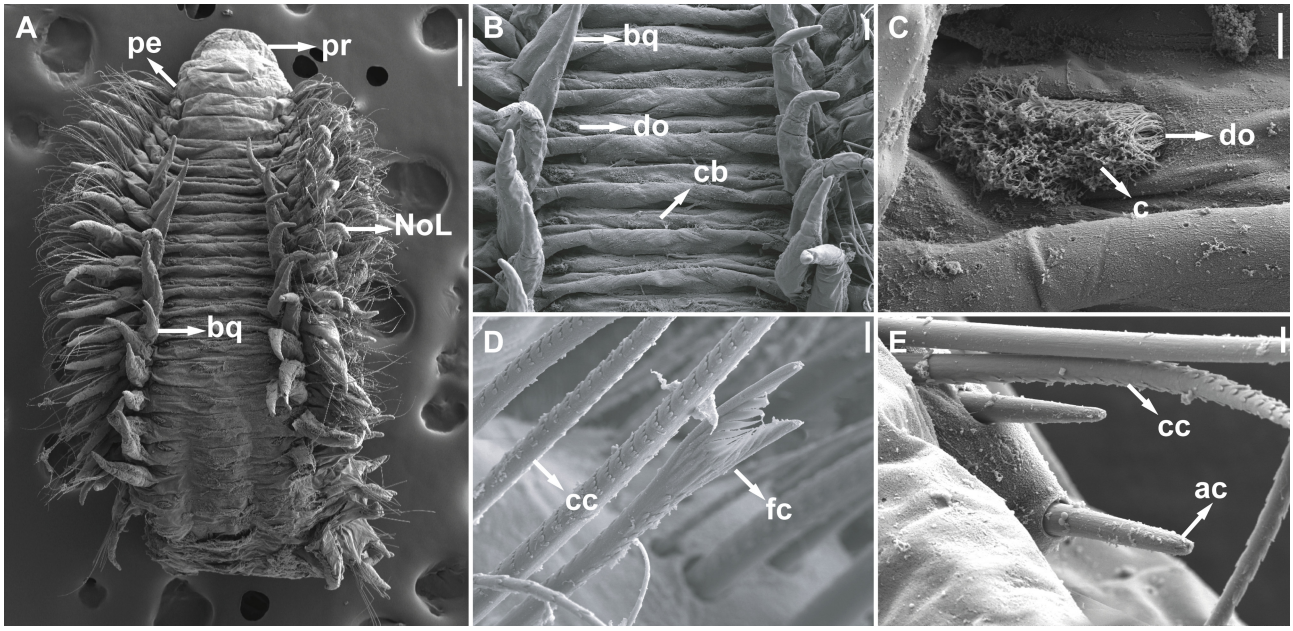

FIGURE 12. *Naineris* sp. examined under SEM (SERC 252000): (A) Anterior end, dorsal view; (B) Thoracic segments, dorsal view; (C) Cilia in dorsal organs; (D) Furcate chaetae in abdominal segment, lateral view; (E) Acicular spines in abdominal segments. bq—branchia, c—dorsal organ cilia, cb—ciliary band, cc—crenulated capillary chaeta, do—dorsal organ, fc—furcate chaeta, NoL—notopodial lobe, pe—peristomium, pr—prostomium. Scale bars; (A): 100 μm; (B): 20 μm; (C): 10 μm; (D–E): 2 μm.

Description. Small specimens, presumably juveniles (Fig. 12A). Color in alcohol light tan. Thorax and abdomen distinct. Prostomium anteriorly rounded (Fig. 12A); eyespots not discernible; nuchal organs present. Peristomium as 1–2 achaetous rings (Fig. 12A); mouth opening located ventrally; proboscis not everted.

Branchiae from chaetiger 6 (Fig. 12A), elongate from first pair. Paired dorsal sensory organs between branchial bases, oval-shaped (Fig. 12B, C). Dorsal crest as ciliary bands from first thoracic segment, straight (Fig. 12B).

Thorax dorsoventrally flattened. Parapodia biramous. Thoracic notopodial and neuropodial lobes lanceolate. Abdominal notopodial and neuropodial lobes triangular.

Thoracic notochaetae with crenulated capillaries only. Abdominal notochaetae including capillaries and furcate chaetae (Fig. 12D); furcate chaetae with unequal tynes and thin needles between; shaft with several transversal rows of 5–7 barbs. Thoracic neurochaetae with capillaries only. Abdominal neurochaetae with capillaries and 1–2 acute acicular spines (Fig. 12E).

Pygidium with terminal anus, bearing anal cirri, presumably four cirri.

Remarks. Based on molecular data, the examined specimens represent an undescribed species. All specimens were of small size, presumably juveniles. The species is unique in having dorsal ciliary bands from the first thoracic segments. However, the species is not formally named here due to a lack of detailed information on the adult definitive morphological characters.

Discussion

This study is the first step toward understanding the genetic and morphological diversity of the *Naineris setosa* complex. The cosmopolitan distribution of *N. setosa* suggested by the earlier studies (Hartman 1951, 1957; Solis-Weiss & Fauchald 1989; Blake & Giangrande 2011; Dean & Blake 2015; Blake 2017) and its stagnated taxonomy over time can partly be explained by the fact that it was the only species of the genus bearing only capillary chaetae in thoracic neuropodia. Nevertheless, after careful examination, several morphological characters consistently differed in the worms from the studied Atlantic and Pacific populations, especially if examined in detail. For instance, the dorsal crest in *N. setosa sensu lato* is usually described in the literature as low. In the present study, we reported that the dorsal crest can vary in shape from straight to lobed, which can also change along the body. In addition, it can be hypertrophied, folded, and bear long cilia such as in *Naineris lanai* sp. n. collected from anoxic mud. At the same time, the species inhabiting regular marine aerated sediments show no such modifications (Blake & Giangrande 2011).

Similarly, we observed that parapodial lobes could be undivided or forked. Forked notopodial lobes were described as a unique character in *Naineris furcillata* Blake, 2017. Nonetheless, this character was also reported in *N. lanai* sp. n., with up to two furcations in some notopodial lobes (Figure 11D–G). Similar structures were reported by Hartman (1957), who described abdominal subpodial lobes in *N. setosa* specimens from the Gulf of Mexico. Solis-Weiss & Fauchald (1989) considered additional lobes a malformation. We suggest that subdivision of the parapodial lobes is characteristic for the specimens from muddy sediments with possibly reduced oxygen levels. According to Glasby *et al*. (2021), parapodial modifications may represent an adaptation to increasing surface area for oxygen uptake in anoxic environments.

Phylogenetic analysis utilizing several unlinked loci can aid in uncovering genetic diversity within complexes of species with similar morphology (Salicini *et al*. 2011; Liu *et al*. 2017; Qiu *et al*. 2020). In the present study, we attempted to delimit the species within the *Naineris setosa* complex by analyzing two mitochondrial and one nuclear marker. Phylogenetic analysis based on the COI marker and the combined dataset of three markers recovered three highly supported clades in the study material. Nevertheless, the individual 16S and 28S gene trees had different topologies. In the 16S analysis, only two clades were recovered, one combining the specimens from the Atlantic and the other from the Pacific. The analysis based on 28S recovered the North Pacific clade sister to the clade representing *N. setosa* s. str. specimens. In contrast, the South and Southeastern Brazil specimens did not form a clade. Similar results were obtained by the haplotype network analysis. Furthermore, the haplotype network of 28S showed the presence of two significantly different haplotypes in the Pacific population, with 9 substitutions present in a generally very conservative nuclear marker.

The interspecific COI distances between the species in the *N. setosa* complex ranged from 13 to 16%, which was comparable with other studies on annelids using COI data for species discrimination (Taboada *et al*. 2015,

2017; Seixas *et al*. 2021). For 16S, the interspecific distances ranged from 0 to 6%, which was considerably lower than in other species complexes of polychaetes (Drennan *et al*. 2019; Radashevsky *et al*. 2020). Still, they were comparable with those in Clitellata (Martinsson *et al*. 2020). All Atlantic specimens shared the same haplotype in 16S, which could be explained by the low evolutionary rates in 16S in the *Naineris setosa* complex and possible recent speciation events between the two Atlantic species. For 28S, the distances ranged from 1.1% to 1.8%, which was similar to other polychaete species complexes (Grosse *et al*. 2020; Radashevsky *et al*. 2020; Kolbasova & Neretina 2021) and can be considered significant, given that 28S evolves at low rates.

Mitonuclear discordance is expected in the animal kingdom (Rokas *et al*. 2003; Toews & Brelsford 2012; Dávalos *et al*. 2012) and was reported for several groups of organisms (Degnan & Rosenberg 2009; Debiasse *et al*. 2014; Hirano *et al*. 2019; Ortiz *et al*. 2021; Formaggioni *et al*. 2022), including annelids (Liu *et al*. 2018; Elgetany *et al*. 2020). Phylogenies reconstruction based on a single marker may conflict as no single gene can capture all nuances of the phylogenetic relationships of a taxon (Rokas *et al*. 2003). In our study, one of the mitochondrial markers, 16S, provided less resolution than COI, indicating low evolutionary rates in the former in *Naineris*. The rates of evolution in different markers are poorly understood. Protein coding and non-coding genes show different evolution rates, which may also differ among codon positions within a coding gene (Liò & Goldman 1998). A phylogenomic approach, combining many genes, may help resolving conflicting topologies (Gee 2003; Rokas *et al*. 2003; Bleidorn 2017).

Even though our findings support that some of the North Pacific populations of the former *Naineris setosa* represent a different species, the Galapagos population reported by Blake (2017) still needs to be studied with well-preserved specimens and molecular data to discard the Amphi-American distribution. Furthermore, a specimen of *Naineris* (identified as *N. australis* collected off Sydney) bearing only capillaries in thoracic neuropodia, paired dorsal organs, and similar parapodial structures was found in the Australian Museum collection (W.22470, unpubl.). After examining numerous specimens of the *Naineris setosa* species complex, we discovered that, in some cases, broken capillary chaetae might strongly resemble uncini, especially in the old specimens (R.A. personal observations). This could probably lead to misidentification of *Naineris* species in scientific collections. Presumably, other similar species were misidentified as *N. setosa* worldwide, requiring further verification and subsequent revision.

We confirmed the Amphi-Atlantic distribution of *Naineris setosa* s. str. with two records reported from the Tyrrhenian and the Ionian Seas. This corroborated the earlier records of the species in the Mediterranean and corroborated its alien status (Blake & Giangrande 2011; Khedhri *et al*. 2014; Atzori *et al*. 2016; Arduini *et al*. 2022; Rebai *et al*. 2022; Struck *et al*. 2023). The species was believed to have been introduced in the Mediterranean Sea due to aquaculture (Blake & Giangrande 2011) and shipping as in the case of possible regional introductions within the Mediterranean (Khedri *et al*. 2014). *Naineris setosa* s. str. can be considered established in the Mediterranean since later records expanded its distribution to Egypt (Struck *et al*. 2023), Tunisia (Khedhri *et al*. 2014; Rebai *et al*. 2022), and the Adriatic (Blake & Giangrande 2011), Ionian (Arduini *et al*. 2022), and Tyrrhenian (Atzori *et al*. 2016) seas. *Naineris setosa* was first reported in Brazil by Nonato (1981); since then, the number of Brazilian records increased (Amaral *et al*. 2006–2022). Even though most of our sampling in Brazil was conducted in bays near the main ports, suggesting shipping as a possible reason for the range expansion, it is hard to determine whether Brazil is part of *N. setosa* s. str. native distribution range or represents a newly colonized area. Further studies, with additional North and Tropical Atlantic samples, including the type locality, may help better understanding of the species' bioinvasive potentials, establish effective monitoring programs in affected areas, and avoid new invasions in susceptible regions.

Availability of data and material: All physical specimens used in this study are kept in the registered scientific collections. All sequences have been submitted to GenBank and BOLD (see Table 1 for accession numbers and BOLD process IDs). Alignments were uploaded to TREEBASE as nexus-formatted data (http://purl.org/phylo/treebase/phylows/study/TB2:S30855).

Acknowledgments

We extend our gratitude to Joana Zanol, Camila Messias (MNRJP), Cecília Amaral (ZUEC-POL), Mônica Petti (ColBIO), Gustav Paulay (FM), Stephen Keable (AM), for the loan of specimens. We thank Karen Osborn (USNM), Lily Berniker (AMNH), Eric Lasso-Wasem and Lourdes Rojas (YPM). We are grateful to Irene Heggstad (Electron

microscopic laboratory at the University of Bergen) for assistance with SEM. RA is deeply indebted to Leslie Harris (LACM) for lodging him during his visit to the LACM and for providing specimens. A special acknowledegement to Tony Phillips for providing materials during the Bodega-Bay BioBlitz (SERC) and to Erica Keppel and Gregory Ruiz for loaning materials from the Invasion lab (SERC) collection. Thanks to Joachim Langeneck for providing ethanol-fixed specimens from the Mediterranean. We also thank Louise Lindblom (UiB) for their help in molecular laboratory work. Christoph Bleidorn and an anonymous reviewer provided valuable comments that improved our manuscript. Finally, not surprisingly, RA would like to dedicate this paper to the memory of the most brilliant scientist Brazil ever produced, Paulo Lana, his late supervisor, whose passion for encouraging new generations was unsurpassed.

Funding

This study was financed in part by the Coordenação de Aperfeiçoamento de Pessoal de Nível Superior - Brasil (CAPES) - (Doctorate fellowship, process number: 88882.382993/2019-01) and CAPES-PRINT-UFPR (Ph. D. Exchange program, process number: 88887.696847/2022-00). RA was also supported by the USNM with the Kenneth Jay Boss Fellowship in Invertebrate Zoology and by the LACM with the Students Collections Study Award. Sampling of Newport Dunes specimens was possible through agreement No.: P1675035 between the California Department of Fish and Wildlife (CDFW) and SERC.

References

Amaral, A.C.Z., Nallin, S.A.H., Steneir, T.M., Forroni, T. de O. & Gomes Filho, D. (2006) *Catálogo das Espécies de Annelida Polychaeta do Brasil*. Available from: http://www.ib.unicamp.br/museu_zoologia/files/lab_museu_zoologia/Catalogo_Polychaeta_Amaral_et_al_2012.pdf (accessed 4 July 2023)

Arduini, D., Borghese, J., Gravina, M. F., Trani, R., Longo, C., Pierri, C. & Giangrande, A. (2022) Biofouling Role in Mariculture Environment Restoration: An Example in the Mar Grande of Taranto (Mediterranean Sea). *Frontiers in Marine Science*, 9, 842616.
https://doi.org/10.3389/fmars.2022.842616

Atzori, G., López, E., Addis, P., Sabatini, A. & Cabiddu, S. (2016) First record of the alien polychaete *Naineris setosa* (Scolecida; Orbiniidae) in Tyrrhenian Sea (Western Mediterranean). *Marine Biodiversity Records*, 9 (1), 1–6.
https://doi.org/10.1186/s41200-016-0017-6

Blainville, H. (1828) *Dictionnaire des Sciences naturelles, dans lequel on traite méthodiquement des différens êtres de la nature, considérés soit en eux-mêmes, d'après l'état actuel de nos connoissances, soit relativement a l'utilité qu'en peuvent retirer la médicine, l'agriculture, le commerce et les arts. Suivi d'une biographie des plus célèbres naturalistes*. FG Levrault, Strasbourg and Paris. [unknown pagination]

Blake, J.A. (2000) A new genus and species of polychaete worm (Family Orbiniidae) from methane seeps in the Gulf of Mexico, interrelationships of the genera of Orbiniidae. *Cahiers de Biologie Marine*, 41 (4), 435–449.
https://doi.org/10.21411/CBM.A.84F1D61E

Blake, J.A. (2017) Polychaeta Orbiniidae from Antarctica, the Southern Ocean, the Abyssal Pacific Ocean, and off South America. *Zootaxa*, 4218 (1), 1–145.
https://doi.org/10.11646/zootaxa.4218.1.1

Blake, J.A. (2020) New species and records of deep-water Orbiniidae (Annelida, Polychaeta) from the Eastern Pacific continental slope, abyssal Pacific Ocean, and the South China Sea. *Zootaxa*, 4730 (1), 1–61.
https://doi.org/10.11646/zootaxa.4730.1.1

Blake, J.A. (2021) New species and records of Orbiniidae (Annelida, Polychaeta) from continental shelf and slope depths of the Western North Atlantic Ocean. *Zootaxa*, 4930 (1), 1–123.
https://doi.org/10.11646/zootaxa.4930.1.1

Blake, J.A. & Giangrande, A. (2011) *Naineris setosa* (Verrill) (Polychaeta, Orbiniidae), an American subtropical-tropical polychaete collected from an aquaculture facility in Brindisi (Adriatic Sea, Italy): A possible alien species. *Italian Journal of Zoology*, 78 (Supplement), 20–26.
https://doi.org/10.1080/11250003.2011.577982

Bleidorn, C. (2005) Phylogenetic relationships and evolution of Orbiniidae (Annelida, Polychaeta) based on molecular data. *Zoological Journal of the Linnean Society*, 144 (1), 59–73.
https://doi.org/10.1111/j.1096-3642.2005.00160.x

Bleidorn, C., Hill, N., Erséus, C. & Tiedemann, R. (2009) On the role of character loss in orbiniid phylogeny (Annelida): Molecules vs. morphology. *Molecular Phylogenetics and Evolution*, 52 (1), 57–69.

https://doi.org/10.1016/j.ympev.2009.03.022
Bleidorn, C. (2017) *Phylogenomics: an introduction*. Springer, Cham, 217 pp.
https://doi.org/10.1007/978-3-319-54064-1
Carr, C.M., Hardy, S.M., Brown, T.M., Macdonald, T.A. & Hebert, P.D.N. (2011) A tri-oceanic perspective: DNA Barcoding reveals geographic structure and cryptic diversity in Canadian polychaetes. *PLoS ONE*, 6 (7), e22232.
https://doi.org/10.1371/journal.pone.0022232
Çinar, M.E. (2013) Alien polychaete species worldwide: current status and their impacts. *Journal of the Marine Biological Association of the United Kingdom*, 93 (5), 1257–1278.
https://doi.org/10.1017/S0025315412001646
Clement, M., Snell, Q., Walker, P., Posada, D. & Crandall, K. (2002) TCS: estimating gene genealogies. *In*: *Proceedings 16th International Parallel and Distributed Processing Symposium, Fort Lauderdale, Florida*, 15–19 April 2002, 0184.
Dávalos, L.M., Cirranello, A.L., Geisler, J.H. & Simmons, N.B. (2012) Understanding phylogenetic incongruence: lessons from phyllostomid bats. *Biological Reviews*, 87 (4), 991–1024.
https://doi.org/10.1111/j.1469-185X.2012.00240.x
Day, J.H. (1961) The polychaet fauna of South Africa. Part 6. Sedentary species dredged off Cape coasts with a few new records from the shore. *Zoological Journal of the Linnean Society*, 44 (299), 463–560.
https://doi.org/10.1111/j.1096-3642.1961.tb01623.x
Day, J.H. (1963) The polychaete fauna of South Africa. Part 8: New species and records from grab samples and dredgings. *Bulletin of the British Museum (Natural History)*, Series Zoology, 10 (7), 381–445.
https://doi.org/10.5962/bhl.part.20530
Day, J.H. (1965) Israel South Red Sea Expedition, 1962, Reports no. 7. Some Polychaeta from the Israel South Red Sea Expedition, 1962. *Bulletin of the Sea Fisheries Research Station*, *Haifa*, 38, 15–27.
Day, J.H. (1977) A review of the Australian and New Zealand Orbiniidae (Annelida: Polychaeta). *In*: *Essays on Polychaetous Annelids in Memory of Dr. Olga Hartman.* Allan Hancock Found, Los Angeles, California, pp. 217–246.
Dean, H.K. & Blake, J.A. (2015) The Orbiniidae (Annelida: Polychaeta) of Pacific Costa Rica. *Zootaxa*, 3956 (2), 183–198.
https://doi.org/10.11646/zootaxa.3956.2.2
DeBiasse, M.B., Nelson, B.J. & Hellberg, M.E. (2014) Evaluating summary statistics used to test for incomplete lineage sorting: mito-nuclear discordance in the reef sponge *Callyspongia vaginalis*. *Molecular Ecology*, 23 (1), 225–238.
https://doi.org/10.1111/mec.12584
Degnan, J.H. & Rosenberg, N.A. (2009) Gene tree discordance, phylogenetic inference and the multispecies coalescent. *Trends in ecology & evolution*, 24 (6), 332–340.
https://doi.org/10.1016/j.tree.2009.01.009
Drennan, R., Wiklund, H., Rouse, G.W., Georgieva, M.N., Wu, X., Kobayashi, G., Yoshino, K. & Glover, A.G. (2019) Taxonomy and phylogeny of mud owls (Annelida: Sternaspidae), including a new synonymy and new records from the Southern Ocean, North East Atlantic Ocean and Pacific Ocean: challenges in morphological delimitation. *Marine Biodiversity*, 49, 2659–2697.
https://doi.org/10.1007/s12526-019-00998-0
Elgetany, A.H., van Rensburg, H., Hektoen, M., Matthee, C., Budaeva, N., Simon, C.A. & Struck, T.H. (2020) Species delineation in the speciation grey zone—The case of *Diopatra* (Annelida, Onuphidae). *Zoologica Scripta,* 49 (4), 516–534.
https://doi.org/10.1111/zsc.12421
Fabricius, O. (1780) *Fauna Groenlandica: systematice sistens animalia Groenlandiae occidentalis hactenus indagata, quoad nomen specificum, triviale, vernaculumque: synonyma auctorum plurium, descriptionem, locum, victum, generationem, mores, usum, capturamque singuli, prout detegendi occasio fuit: maximaque parte secundum proprias observationes*. Impensis Ioannis Gottlob Rothe, Hafniae, XIV + 450 pp.
https://doi.org/10.5962/bhl.title.13489
Formaggioni, A., Plazzi, F. & Passamonti, M. (2022) Mito-nuclear coevolution and phylogenetic artifacts: the case of bivalve mollusks. *Scientific Reports*, 12 (1), 11040.
https://doi.org/10.1038/s41598-022-15076-y
Gee, H. (2003) Ending incongruence. *Nature*, 425 (6960), 782–782.
https://doi.org/10.1038/425782a
Glasby, C.J., Erséus, C. & Martin, P. (2021) Annelids in extreme aquatic environments: Diversity, adaptations and evolution. *Diversity*, 13 (2), 1–23.
https://doi.org/10.3390/d13020098
Grosse, M., Bakken, T., Nygren, A., Kongsrud, J.A. & Capa, M. (2020) Species delimitation analyses of NE Atlantic *Chaetozone* (Annelida, Cirratulidae) reveals hidden diversity among a common and abundant marine annelid. *Molecular phylogenetics and evolution,* 149, 106852.
https://doi.org/10.1016/j.ympev.2020.106852
Grube, A.E. (1855) Beschreibungen neuer oder wenig bekannter Anneliden. *Archiv fur Naturgeschichte*, *Berlin*, 21, 81–128.
https://doi.org/10.5962/bhl.part.13989
Hartman, O. (1942) A review of the types of polychaetous annelids at the Peabody Museum of Natural History, Yale University. *Bulletin of the Bingham Oceanographic Collections*, 8, 1–98.

Hartman, O. (1951) The littoral marine annelids of the Gulf of Mexico. *Publications of the Institute of Marine Science, University of Texas*, 2, 7–124.
Hartman, O. (1957) Orbiniidae, Apistobranchidae, Paraonidae and Logosomidae. *Allan Hancock Pacific Expeditions*, 15 (3), 211–393, pls. 20–44.
Hillis, D.M. & Dixon, M.T. (1991) Ribosomal DNA: molecular evolution and phylogenetic inference. *The Quarterly review of biology,* 66 (4), 411–453.
https://doi.org/10.1086/417338
Hirano, T., Saito, T., Tsunamoto, Y., Koseki, J., Ye, B., Do, V.T, Miura, O., Suyama, Y. & Chiba, S. (2019) Enigmatic incongruence between mtDNA and nDNA revealed by multi-locus phylogenomic analyses in freshwater snails. *Scientific Reports*, 9 (1), 1–13.
https://doi.org/10.1038/s41598-019-42682-0
Hoang, D.T., Chernomor, O., Von Haeseler, A., Minh, B.Q. & Vinh, L.S. (2018) UFBoot2: improving the ultrafast bootstrap approximation. *Molecular biology and evolution*, 35 (2), 518–522.
https://doi.org/10.1093/molbev/msx281
Hutchings, P. & Kupriyanova, E. (2018) Cosmopolitan polychaetes—Fact or fiction? Personal and historical perspectives. *Invertebrate systematics*, 32 (1), 1–9.
https://doi.org/10.1071/IS17035
Kalyaanamoorthy, S., Minh, B.Q., Wong, T.K., Von Haeseler, A. & Jermiin, L.S. (2017) ModelFinder: fast model selection for accurate phylogenetic estimates. *Nature methods*, 14 (6), 587–589.
https://doi.org/10.1038/nmeth.4285
Katoh, K., Kuma, K.I., Toh, H. & Miyata, T. (2005) MAFFT version 5: Improvement in accuracy of multiple sequence alignment. *Nucleic Acids Research*, 33, 511–518.
https://doi.org/10.1093/nar/gki198
Khedhri, I., Lavesque, N., Bonifácio, P., Djabou, H. & Afli, A. (2014) First record of *Naineris setosa* (Verrill, 1900) (Annelida: Polychaeta: Orbiniidae) in the Western Mediterranean Sea. *BioInvasions Records*, 3 (2), 83–88.
https://doi.org/10.3391/bir.2014.3.2.05
Kinberg, J.G.H. (1867) Annulata nova. *Öfversight af Kungliga Vetenskaps-Adakemiens Förhandlingar, Stockholm*, 22, 239–258.
Kolbasova, G. & Neretina, T. (2021) A new species of *Pelagobia* (Lopadorrhynchidae, Annelida), with some notes on literature records of *Pelagobia longicirrata* Greeff, 1879. *Zootaxa*, 5023 (1), 77–92.
https://doi.org/10.11646/zootaxa.5023.1.4
Kumar, S., Stecher, G., Li, M., Knyaz, C. & Tamura, K. (2018) MEGA X: molecular evolutionary genetics analysis across computing platforms. *Molecular biology and evolution*, 35 (6), 1547.
https://doi.org/10.1093/molbev/msy096
Kvist, S. (2016) Does a global DNA barcoding gap exist in Annelida? *Mitochondrial DNA Part A*, 27 (3), 2241–2252.
https://doi.org/10.3109/19401736.2014.984166
Leigh, J.W. & Bryant, D. (2015) POPART: full-feature software for haplotype network construction. *Methods in ecology and evolution*, 6 (9), 1110–1116.
https://doi.org/10.1111/2041-210X.12410
Liò, P. & Goldman, N. (1998) Models of molecular evolution and phylogeny. *Genome research*, 8 (12), 1233–1244.
https://doi.org/10.1101/gr.8.12.1233
Liu, Y., Fend, S. V., Martinsson, S., Luo, X., Ohtaka, A. & Erséus, C. (2017) Multi-locus phylogenetic analysis of the genus *Limnodrilus* (Annelida: Clitellata: Naididae). *Molecular Phylogenetics and Evolution*, 112, 244–257.
https://doi.org/10.1016/j.ympev.2017.04.019
Liu, P., Xu, L., Xu, S. L., Martínez, A., Chen, H., Cheng, D., Dumont, H., Han, B-P. & Fontaneto, D. (2018) Species and hybrids in the genus *Diaphanosoma* Fischer, 1850 (Crustacea: Branchiopoda: Cladocera). *Molecular phylogenetics and evolution*, 118, 369–378.
https://doi.org/10.1016/j.ympev.2017.10.016
Martinsson, S., Klinth, M. & Erséus, C. (2020) Testing species hypotheses for *Fridericia magna*, an enchytraeid worm (Annelida: Clitellata) with great mitochondrial variation. *BMC Evolutionary Biology*, 20 (1), 1–12.
https://doi.org/10.1186/s12862-020-01678-5
Meyer, A., Bleidorn, C., Rouse, G.W. & Hausen, H. (2008) Morphological and molecular data suggest a cosmopolitan distribution of the polychaete *Proscoloplos cygnochaetus* Day, 1954 (Annelida, Orbiniidae). *Marine Biology*, 153, 879–889.
https://doi.org/10.1007/s00227-007-0860-4
Minh, B.Q., Schmidt, H.A., Chernomor, O., Schrempf, D., Woodhams, M.D., Von Haeseler, A. & Lanfear, R. (2020) IQ-TREE 2: new models and efficient methods for phylogenetic inference in the genomic era. *Molecular biology and evolution*, 37 (5), 1530–1534.
https://doi.org/10.1093/molbev/msaa015
Müller, F. (1858) Einiges über die Annelidenfauna der Insel Santa Catharina an der brasilianischen Küste. *Archiv für Naturgeschichte*, 24 (1), 211–220.
Nonato, E.F. (1981) *Contribuição ao conhecimento dos anelídeos poliquetas bentônicos da Plataforma Continental Brasileira,*

entre Cabo Frio e o Arroio Chuí. Livre Docência Thesis, Universidade de São Paulo, São Paulo, 246 pp.
Nonato, E.F., Bolívar, G.A. & Lana, P. (1986) *Laonice branchiata*, a new species of Spionidae (Annelida; Polychaeta) from the southeastern Brazilian coast. *Revista Nerítica*, 1 (3), 22–25.
https://doi.org/10.5380/rn.v1i3.41193
Ortiz, D., Pekár, S., Bilat, J. & Alvarez, N. (2021) Poor performance of DNA barcoding and the impact of RAD loci filtering on the species delimitation of an Iberian ant-eating spider. *Molecular phylogenetics and evolution*, 154, 106997.
https://doi.org/10.1016/j.ympev.2020.106997
Palumbi, S.R., Martin, A., Romano, S., McMillan, W.O., Stice, L. & Grabowski, G. (1991) *The simple fool's guide to PCR, Special Publication.* Department of Zoology and Kewalo Marine Laboratory, University of Hawaii, Honolulu, 28 pp.
Qiu, P. L., Liu, S. Y., Bradshaw, M., Rooney-Latham, S., Takamatsu, S., Bulgakov, T. S., Tang, S.R., Feng, J., Aroge, T., Li, Y., Wang, L.L. & Braun, U. (2020) Multi-locus phylogeny and taxonomy of an unresolved, heterogeneous species complex within the genus *Golovinomyces* (Ascomycota, Erysiphales), including *G. ambrosiae*, *G. circumfusus* and *G. spadiceus*. *BMC microbiology*, 20, 1–16.
https://doi.org/10.1186/s12866-020-01731-9
Radashevsky, V.I. & Lana, P. (2009) *Laonice* (Annelida: Spionidae) from South and Central America. *Zoosymposia*, 2, 265–295.
https://doi.org/10.11646/zoosymposia.2.1.19
Radashevsky, V.I., Malyar, V.V., Pankova, V.V., Gambi, M.C., Giangrande, A., Keppel, E., Nygren, A., Al-Kandari, M. & Carlton, J.T. (2020) Disentangling invasions in the sea: molecular analysis of a global polychaete species complex (Annelida: Spionidae: *Pseudopolydora paucibranchiata*). *Biological Invasions*, 22 (12), 3621–3644.
https://doi.org/10.1007/s10530-020-02346-x
Rebai, N., Mosbahi, N., Dauvin, J.C. & Neifar, L. (2022) Ecological Risk Assessment of Heavy Metals and Environmental Quality of Tunisian Harbours. *Journal of Marine Science and Engineering*, 10 (11), 1625.
https://doi.org/10.3390/jmse10111625
Rioja, E. (1960) Estudios anelidologicos. XXIV. Adiciones a la fauna de Anelidos Poliquetos de las costas orientales de México. *Anales Del Instituto de Biología, México*, 31, 289–316.
Rokas, A., Williams, B.L., King, N. & Carroll, S.B. (2003) Genome-scale approaches to resolving incongruence in molecular phylogenies. *Nature*, 425 (6960), 798–804.
https://doi.org/10.1038/nature02053
Salicini, I., Ibáñez, C. & Juste, J. (2011) Multilocus phylogeny and species delimitation within the Natterer's bat species complex in the Western Palearctic. *Molecular Phylogenetics and Evolution*, 61 (3), 888–898.
https://doi.org/10.1016/j.ympev.2011.08.010
Seixas, V.C., Steiner, T.M., Solé-Cava, A.M., Amaral, A.C.Z. & Paiva, P.C. (2021) Hidden diversity within the *Diopatra cuprea* complex (Annelida: Onuphidae): Morphological and genetics analyses reveal four new species in the south-west Atlantic. *Zoological Journal of The Linnean Society*, 191 (3), 637–671.
https://doi.org/10.1093/zoolinnean/zlaa032
Solis-Weiss, V. & Fauchald, K. (1989) Orbiniidae (Annelida: Polychaeta) from mangrove root-mats in Belize, with a revision of the protoariciin genera. *Proceedings of the Biological Society of Washington*, 102 (3), 772–792.
Struck, T. H., Golombek, A., Hoesel, C., Dimitrov, D. & Elgetany, A.H. (2023) Mitochondrial Genome Evolution in Annelida—A Systematic Study on Conservative and Variable Gene Orders and the Factors Influencing its Evolution. *Systematic Biology*, syad023.
https://doi.org/10.1093/sysbio/syad023
Taboada, S., Riesgo, A., Bas, M., Arnedo, M. A., Cristobo, J., Rouse, G.W. & Avila, C. (2015) Bone-eating worms spread: insights into shallow-water *Osedax* (Annelida, Siboglinidae) from Antarctic, Subantarctic, and Mediterranean waters. *PLoS One*, 10 (11), e0140341.
https://doi.org/10.1371/journal.pone.0140341
Taboada, S., Leiva, C., Bas, M., Schult, N. & McHugh, D. (2017) Cryptic species and colonization processes in *Ophryotrocha* (Annelida, Dorvilleidae) inhabiting vertebrate remains in the shallow-water Mediterranean. *Zoologica Scripta*, 46 (5), 611–624.
https://doi.org/10.1111/zsc.12239
Tamura, K., Stecher, G. & Kumar, S. (2021) MEGA11: molecular evolutionary genetics analysis version 11. *Molecular Biology and Evolution*, 38 (7), 3022–3027.
https://doi.org/10.1093/molbev/msab120
Toews, D.P. & Brelsford, A. (2012) The biogeography of mitochondrial and nuclear discordance in animals. *Molecular ecology*, 21 (16), 3907–3930.
https://doi.org/10.1111/j.1365-294X.2012.05664.x
Treadwell, A.L. (1901) The polychaetous annelids of Porto Rico. *Bulletin of the United States National Fish Commission*, 20 (2), 183–210.
Treadwell, A.L. (1936) Polychaetous annelids from the vicinity of Nonsuch Island, Bermuda. *Zoologica*, 21 (1), 49–68.
https://doi.org/10.5962/p.190351
Treadwell, A.L. (1939) Polychaetous annelids from Porto Rico and vicinity. *In*: *Scientific Survey of Porto Rico and the Virgin*

Islands. Vol. 16. New York Academy of Sciences, New York, New York, pp. 151–319.
Verril, A.E. (1900) Additions to the Turbellaria, Nemertina and Annelida of the Bermudas, with revisions of some New England genera and species. *Transactions of the Connecticut Academy of Arts and Sciences*, 10, 595–671. https://doi.org/10.5962/bhl.part.7035
Zhadan, A., Stupnikova, A. & Neretina, T. (2015) Orbiniidae (Annelida: Errantia) from Lizard Island, Great Barrier Reef, Australia with notes on orbiniid phylogeny. *Zootaxa*, 4019 (1), 773–801. https://doi.org/10.11646/zootaxa.4019.1.27
Zhadan, A. (2020) Review of Orbiniidae (Annelida, Sedentaria) from Australia. *Zootaxa*, 4860 (4), 451–502. https://doi.org/10.11646/zootaxa.4860.4.1
Zhang, J., Kapli, P., Pavlidis, P. & Stamatakis, A. (2013) A general species delimitation method with applications to phylogenetic placements. *Bioinformatics*, 29 (22), 2869–2876. https://doi.org/10.1093/bioinformatics/btt499